Greenhouse Gases
Selected Case Studies

Edited by Andrew J. Manning

GREENHOUSE GASES - SELECTED CASE STUDIES

Edited by **Andrew J. Manning**

Greenhouse Gases - Selected Case Studies
http://dx.doi.org/10.5772/61589
Edited by Andrew J. Manning

Contributors

Maria Do Carmo Rangel, Pradeep Kumar Malik, Adrian Ioana, Augustin Semenescu, Christine Chan

Notice

Statements and opinions expressed in the chapters are these of the individual contributors and not necessarily those of the editors or publisher. No responsibility is accepted for the accuracy of information contained in the published chapters. The publisher assumes no responsibility for any damage or injury to persons or property arising out of the use of any materials, instructions, methods or ideas contained in the book.

We are IntechOpen,
the world's leading publisher of
Open Access books
Built by scientists, for scientists

3,800+
Open access books available

116,000+
International authors and editors

120M+
Downloads

151
Countries delivered to

Our authors are among the
Top 1%
most cited scientists

12.2%
Contributors from top 500 universities

Interested in publishing with us?
Contact book.department@intechopen.com

Numbers displayed above are based on latest data collected.
For more information visit www.intechopen.com

Meet the editor

Professor Andrew J. Manning is a Principal Scientist at HR Wallingford Ltd in the Coasts & Estuaries Group (UK), a Professor specializing in Sediment Dynamical Processes at the University of Hull, and a Lecturer in Coastal & Shelf Physical Oceanography at the University of Plymouth (UK). His main area of research is cohesive sediment dynamics in aquatic environments. He completed his degree with honours in Civil Engineering at Polytechnic South West (UK), which was followed by a postgraduate diploma in Hydrographic Surveying, a Master's degree in Applied Marine Science, and a doctorate in Cohesive Sediment Dynamics, all from the University of Plymouth (UK). He is a Fellow of the Royal Geographical Society and was awarded a Vice Chancellor's Research Fellowship in 2007. His research interests include: sediment transport processes, oceanographic instrument development, and estuarine & coastal hydrodynamics. He has supervised graduates, postgraduates and doctoral students focusing on research in marine science. To date he has been a contributing author to more than 90 peer reviewed scientific articles and over 100 articles in refereed international conference proceedings. He has led numerous research projects investigating sediment dynamics in aquatic environments around the world.

Contents

Preface

Greenhouse Gases - Selected Case Studies, is a book which covers a range of topics. The long-term effective management of the natural environment, requires a detailed understanding of greenhouse gases. This has both environmental and economic implications, especially where there is any anthropogenic involvement. Numerical models are often the tool and framework used for predicting the effects, both in the long-term and short-term, of greenhouse gases. However, the relevant atmospheric processes can vary quite considerably depending upon the spatial and temporal scales under consideration.

For this reason for the past few decades, scientists, engineers, meteorologists and mathematicians have all been continuing to conduct research into the many aspects which influence greenhouse gases. These issues range from: industrial science, agricultural research, carbon dioxide and other emissions. It is a pleasure to write the preface to this book published by InTech. It comprises 4 chapters written by international group of research scientists, who specialise in areas such as: energy production, emissions from livestock, chemical industry, and metallurgical process technology.

The majority of the chapters are concerned with gas emission effects. For example: greenhouse gas emissions from livestock; the effect of dopants on the properties of zirconia-supported iron catalysts for ethylbenzene dehydrogenation with carbon dioxide; human health impacts due to heavy metal emissions from a conventional lignite coal-fired electricity generation station, with post-combustion, and oxy-fuel combustion capture technologies; and the treatment of gas emissions through the concept of the environment recycling energy (ERE) in the Romanian steel industry. All authors are responsible for their views and subsequent concluding statements.

In summary, this book provides a selection of case studies on recent research on greenhouse gases, particularly from an interdisciplinary perspective. I would like to thank all of the authors for their contributions and I highly recommend this textbook to both scientists and engineers who deal with the related issues.

Andrew J. Manning
Department of Geography, Environment and Earth Sciences, University of Hull, Hull, UK
School of Marine Science and Engineering, Plymouth University, Plymouth, UK
HR Wallingford, Wallingford, UK

GHG Emissions from Livestock: Challenges and Ameliorative Measures to Counter Adversity

Pradeep Kumar Malik, Atul Purushottam Kolte,
Arindam Dhali, Veerasamy Sejian,
Govindasamy Thirumalaisamy, Rajan Gupta and
Raghavendra Bhatta

Additional information is available at the end of the chapter

Abstract

Livestock and climate change are interlinked through a complex mechanism and serve the role of both contributor as well as sufferer. The livestock sector is primarily accountable for the emission of methane and nitrous oxide. Methane emission takes place from both enteric fermentation and manure management; whilst nitrous oxide emission is purely from manure management. Rumen methanogenesis due to emission intensity and loss of biological energy always remains a priority for the researchers. Greenhouse gas (GHG) emissions from manure are determined by storage conditions and the organic content of the manure waste. Due to large livestock population, India is a major contributor of enteric methane emission, while its contribution to the excrement methane is negligible. In this chapter, information pertaining to enteric methane emission, excrement methane and nitrous oxide emissions and ameliorative/precautionary measures for reducing the intensity of emissions have been compiled and presented.

Keywords: greenhouse gas, GHG mitigation, livestock, methane, nitrous oxide

1. Introduction

Annual greenhouse gas (GHG) emission in 2005 was about 49 gigatonnes (Gt), wherein China contributed the maximum, followed by the United States of America and the European Union

27 [1]. The contribution of India to the total emission is about 4.25% (**Figure 1**). Worldwide livestock are integral component of agriculture and support the livelihood of billions by fulfilling 13% of energy and 28% of protein requirement. Due to the rapid change in food habits, the global demand for milk, meat and eggs in 2050 with reference to year 1990, is expected to increase 30, 60 and 80%, respectively. This additional demand will be met from livestock either by increasing their number or by intensifying productivity. The bovine and ovine population is expected to grow up at a rate of 2.6 and 2.7%, respectively, during next 35 years.
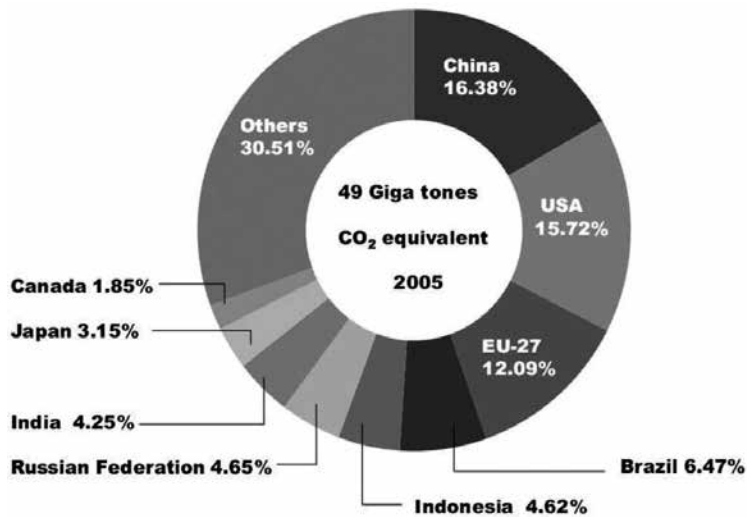
Figure 1. Nation wise greenhouse gas emissions [2] (Reprinted with permission from Takahashi [2]).

Livestock and climate change are inter-hooked in a complex mechanism where adversity of one affects another. Adverse impact of climate change on livestock across the globe will be stratified in accordance with the prevailing agro-climatic conditions. The climatic variation influences livestock in both direct and indirect ways and alterations in ambience (stresses), qualitative and quantitative changes in fodder crops, health are few of them. We can consider the livestock as one of the culprit for climate change and also the sufferer due to negative consequences of changing climate on the productive and reproductive performances of the animal. Elaborating the adverse impact of climate change on livestock production is beyond the scope of chapter and discussed elsewhere in the book. This chapter would focus primarily on the role of livestock in greenhouse gas emissions and ameliorative/precautionary measures for countering the adverse impact.

2. GHG emissions from livestock

Carbon dioxide (CO_2), methane (CH_4), and nitrous oxide (N_2O) are three major GHG emissions from livestock into the atmosphere. However, CO_2 being the part of continuous biological

system cycling is not taken into consideration while calculating total GHG emission from livestock [3]. After power and land use change, agriculture including livestock is the third sector responsible for largest greenhouse gases emission. GHG emissions from different sectors are presented in **Figure 2**. Agriculture as such contributes 14% to the global GHG emissions. Of the total agricultural emissions, 38% is contributed from the soil where N_2O is one of the major GHG. GHG emission from enteric fermentation is also equally large and constitutes 32% of the total GHG emission from agriculture (**Figure 3**). In addition, rice cultivation, biomass burning, and manure management also contribute significantly and make about 30% of the agricultural emissions.
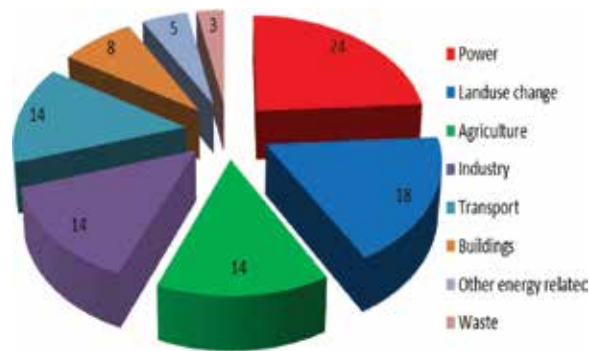
Figure 2. Sector wise GHG emissions.
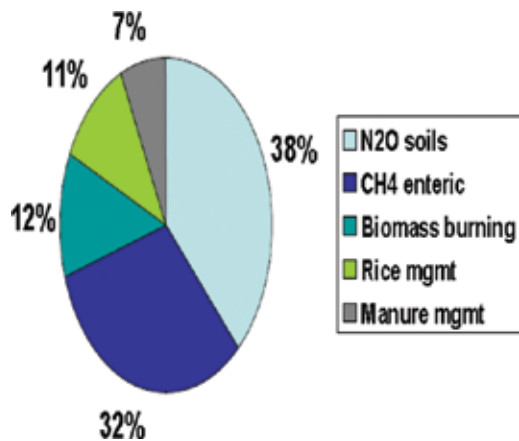
Figure 3. Global agricultural GHG emission.

Livestock emits methane both from enteric fermentation and from manure management; whilst nitrous oxide emission is purely associated with the manure management system. However, methane emission from manure management is far less than the emission from enteric fermentation. Methane emission from excrement is mainly confined to animal man-

agement operations where excrement is handled in liquid based systems. N_2O emission from manure management varies significantly between types of management system and also related to indirect emissions from other forms of nitrogen. Of the total anthropogenic methane and nitrous oxide emissions, livestock globally contribute 35 and 65% of the respective GHGs. Latin America occupies first position (23%) in the list of top enteric methane emitting countries (**Figure 4**), while Africa (14%) and China (13%) hold second and third positions. India stands at the fourth position and is accountable for 11% of the worldwide enteric methane emission (**Figure 4**). The contribution from Middle East and Eastern Europe is negligible and contributes only 2.8% of the total emission [4]. The United States' Environmental Protection Agency [5] projected that the enteric methane emission will substantially increase in 2020 and 2030 in comparison to 2010 (**Figure 5A**). Similarly, projections also imply an increase in enteric methane emission from Indian livestock than that was in 2010. However, methane and nitrous oxide emission will almost remain stabilized for the next 10–20 years (**Figure 5**).
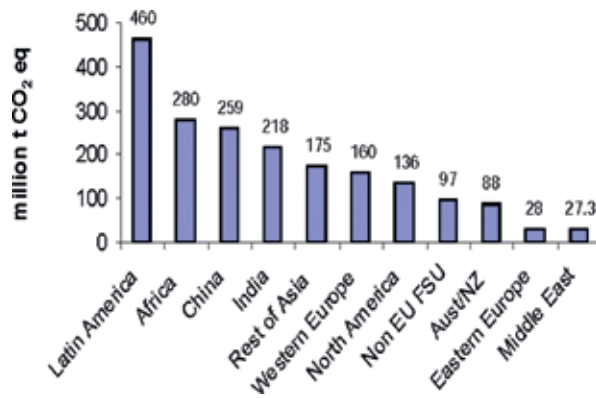
Figure 4. Region wise enteric methane emission [4].
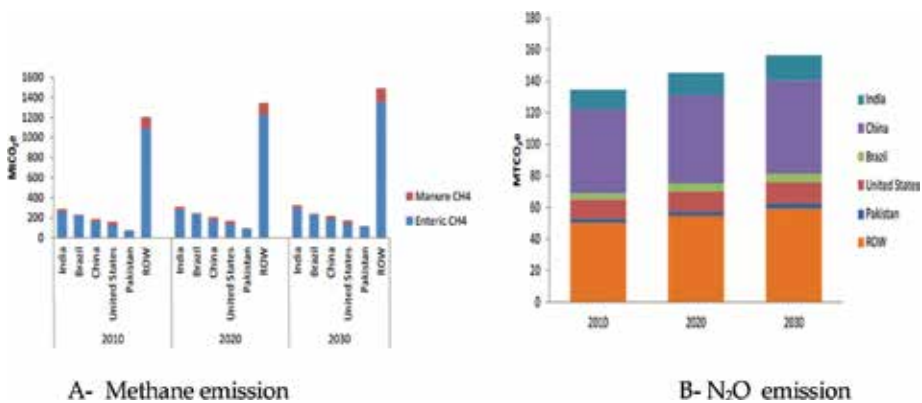
Figure 5. Projections for 2020 and 2030 [5]. (A) Methane emission. (B) N_2O emission.

2.1. Rumen methanogenesis: good and bad associated with it

Rumen harbours a diverse group of microbes that undertake different functions from complex carbohydrate degradation to the removal of end metabolites arise from fermentation. These microbes work in a syntrophic fashion under strict anaerobic conditions and help each other in performing their functions. H_2 is a central metabolite produced in large volume from fermentation and need to be disposed off away from the rumen. Many hydrogenotrophic pathways, such as methanogenesis, reductive acetogenesis, sulfate reduction, and nitrate reduction, have been described as a sink for H_2 in the rumen. Under normal rumen functioning, methanogenesis due to the thermodynamic efficiency is the most prominent hydrogenotrophic pathway. In methanogenesis, H_2 is used for the reduction of CO_2 and conversion into methane which later on eructate from the rumen. Methanogenesis removes unwanted and fatal products of fermentation from the rumen, therefore, it is an essential pathway for the normal rumen functioning, involving the residing microbes and the host animal. The methane energy value is 55.65 MJ/kg [6] and therefore its removal deprives the host animal from a substantial fraction of ingested biological energy. This loss generally lies in the range of 6–12% of the intake [7]. In addition, enteric methane emission due to its high global warming potential (25 times of CO_2) also contributes significantly to the global warming [5]. Due to many intact disadvantages with enteric methane emission, its amelioration up to a desirable extent is much more important than any other GHG. Its relatively shorter half-life offers added opportunity to stabilize global warming in short time and meanwhile other GHG could also be tackled.

2.2. Enteric methane emission: Indian scenario

Various agencies reported quite variable figures for enteric methane emission from Indian livestock. Many have reported annual emission as high as 18 Tg per year, while others have estimated only 7 Tg (**Figure 6**). The average of these estimates comes around 8–10 Tg per year which constitutes about 11% of the global enteric methane emission. India possesses 512 million livestock [8] wherein cattle and buffaloes are the prominent species and make up to 60% of the total livestock in the country.

One of the reasons for high enteric methane emission from India is the larger bovine population which emits more methane than any other livestock species. On an average, cattle and buffaloes aggregately emits more than 90% of the total enteric methane emission of the country. The contribution from small ruminants is relatively small and constitutes only 7.7%. Rest of the methane emissions arise from the species such as yak and mithun, which are scattered to specific states only. Enteric methane emission from crossbred cattle is comparatively much more than the emissions from indigenous cattle (46 versus 25 kg/animal/year). Enteric methane emission from livestock is not uniform across the states and varies considerably according to the livestock numbers, species, type of feed and fodders, etc. The National Institute of Animal Nutrition and Physiology (NIANP), Bangalore has developed an inventory for state wise enteric methane emission from Indian livestock using 19th livestock census report. The NIANP estimates revealed Uttar Pradesh as the largest enteric methane emitting state of the country [9]. Other major methane emitting states in the country are Rajasthan, Madhya Pradesh, Bihar, West Bengal, Maharashtra, Karnataka and Andhra Pradesh (**Figure 7**). These states altogether

holds 66% of the livestock population and accountable for 68% enteric methane emissions. Due to large contribution, these states can be considered as hotspots for reducing enteric methane emissions from livestock and are given priority for tackling the emission.
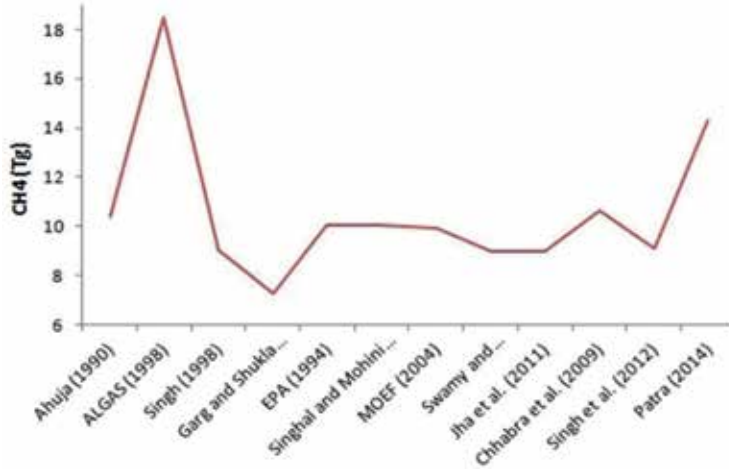

Figure 6. Disparity in enteric methane emission from Indian livestock.

Figure 7. Major enteric methane emitting states in India.

2.3. Enteric methane amelioration: challenges and opportunities

Attempting enteric methane mitigation without understanding necessity, knowing exact emission from country/state, extent and feasibility of reduction, complexity of ruminal microbes and their syntrophic relationship will not serve the effective and sustainable reduction in long term as learnt from past experience in many countries. Archaea in the rumen are methane producing microbes. Earlier methanogens were considered under bacterial domain (prokaryotes), but recent classification by Woese [10] placed them in a distinct domain, which is remarkably different from bacteria. Methanogens archaea are primarily hydrogeno-trophic microbes, which utilize H_2 as the main substrate for methanogenesis. Though, they can Use other substrates also for methanogenesis, but H_2 remains a central metabolite and its partial pressure determines the degree of methanogenesis [11]. Due to its main role in maintaining the redox-potential (reducing environment) of rumen, H_2 is referred as *currency of fermentation* [11]. Therefore, deep understanding of rumen archaea, their substrate require-ment and role in methanogenesis is pre-requisite for achieving sustainable reduction in methane emission. The latest metagenomic approaches served as potential tool and helped in exploring many more cultured and uncultured rumen methanogens for better understanding. The effectiveness and persistency of the ameliorative approach depends on the extent of methanogens being targeted by the approach under investigation. In spite of initial reduction, enteric methane emission usually gets back to the normal level, which is due to partial targeting of methanogen community in rumen. All possible ameliorative measures for enteric methane mitigation are presented in **Table 1**.

Measures	Opportunities/Limitation	Remarks
Reducing the livestock numbers	Due to high number of low producing or non-producing ruminants methane emission per kg of livestock product is high. Killing of such livestock is not possible due to the ban on cow slaughter in the country.	Low productive animals should be graded up with rigorous selection for improving their productivity and less enteric methane emission.
Feeding of quality fodders, concentrate	Feed interventions are the best option for methane amelioration. The uninterrupted availability is a question mark. Area under pasture and permanent fodder production declining or stagnant since last three decades. Livestock are getting their fodders from 7–8% of the arable area in the country.	Improving quality fodders availability seems unrealistic under ever increasing human population and food-feed-fuel competition scenario.
Ionophore	Selective inhibition of microbes and failure to achieve the reduction in long term are big issues. Animals turn back to normal level of emission after short time. Their use is banned in many European countries.	May be tried in rotation as well in combination for sustaining the reduction in long term.
Ration balancing	Ration balancing with feed resources available at farmer's doorstep will improve the productivity with concurrent methane reduction at a low input level.	Farmers need to be made aware about the importance of ration balancing and monetary advantages from the same.

Measures	Opportunities/Limitation	Remarks
Removal of protozoa	Removal of ciliate protozoa from the rumen results in lower methane production. May witness less fibre digestibility. It is practically impossible to maintain protozoa free ruminants.	In spite of complete removal, partial defaunation may be achieved for enteric methane reduction without affecting the fibre digestion.
Reductive acetogenesis	Thermodynamics favour methanogenesis in the rumen. The affinity of acetogens for H_2 substrate is considerably lower than methanogens. It cannot work until and unless target methanogens are absent in the rumen.	Reductive acetogenesis may be promoted by simultaneously targeting rumen archaea. This will ensure less methane with additional acetate availability for the host animal.
Use of plant secondary metabolites	Under the quality fodders deficit scenario, use of PSM as methane mitigating agents is a good option. Dose optimization and validation of methane migration potential *in vivo* on a large scale is mandatory before recommendation.	Inclusion at a safe level without affecting the feed fermentability may be a viable option for enteric methane amelioration. Studies are warranted for assessing the combined action of PSM on *in vivo* methane emission.
Nitrate/Sulfate	Nitrate and sulfate hold the potential to reduce methane emission to a greater extent. These reductive processes are thermodynamically more favourable than methanogenesis. The end product from this productive process will not have any energetic gain for the animal. Intermediate products are toxic to the host animal.	Probably slow releasing sources for these compounds will reduce the toxicity chances caused by intermediate metabolites. A safe level of inclusion must be decided and tested on large number of animals by considering all the species accountable for methane emission.
Active immunization	This approach hold the potential for substantial methane reduction provided methanogen archaea of rumen is explored to a maximum extent for identifying the target candidate for the inclusion in vaccine.	Information on the species and bio-geographic variation in methanogenic archaeal community should be explored for considering this approach for enteric methane amelioration.
Disabling of surface proteins	It is well established that methanogens adhere to the surface of other microbes for H_2 transfer through surface proteins. Identifying and disabling of these surface proteins will certainly reduce enteric methane emission by cutting the supply of H_2.	This is an unexplored area and need some basic and advance research for exploring the possibility.
Biohydrogentation	Restricting the H_2 supply to methanogens through alternate use in bio-hydrogenation, decrease enteric methane amelioration. Use of fat/lipids at a high level depresses fibre digestion. Of the total, only about 5–7% of H_2 is utilized in this process.	This approach is not practical due to high cost of fat/lipids and fibre depression at a high level of use.

Table 1. Ameliorative measures for enteric methane mitigation.

2.4. Plant secondary metabolites as ameliorating agent

Plant secondary metabolites (PSMs) are organic compounds that are not directly involved in the growth, development, or reproduction, but play an important role in plant defence against herbivores. Plant secondary metabolites, on the basis of their biosynthetic origins can be grouped into three: flavonoids, and allied phenolic and polyphenolic compounds; terpenoids and nitrogen-containing alkaloids; and sulphur-containing compounds. Among these, tannins are most important for enteric methane amelioration. Chemically, they are polyphenolic compounds with varying molecular weights, and have the ability to bind natural polymers, such as proteins and carbohydrates. Based on their molecular structure, tannins are classified as either hydrolysable tannins (HT; polyesters of gallic acid and various individual sugars) or condensed tannins (CT; polymers of flavonoids), although there are also tannins that represent combinations of these two basic structures. As PSMs are integral components of abundant phyto-sources and are required in very limited quantity for exerting anti-methanogenic action, therefore, using them as an ameliorating agent would cost very little to the stakeholders.

The tannins exert their anti-methanogenic activity through direct inhibition of methanogen archaea or indirectly by interfering with protozoa and restricting the interspecies H_2 transfer [12, 13]. More than 100 phyto-sources have been evaluated in our laboratory (*in vitro)* for determining their methane mitigation potential and to optimize their level of inclusion in the animal diet [14, 15].

Saponin is another group of plant secondary metabolites that possess a carbohydrate moiety attached to an aglycone, usually steroid or triterpenoid. Saponins are widely distributed in the plant kingdom and research revealed the use of saponin as such or as phyto source legumes that contain an appreciable amount of saponins. Malik and Singhal [16] in an *in vitro* study reported 29% reduction in methane production on the addition of 4% commercial grade saponin in wheat straw and concentrate based diet. Further, same authors [17] also reported a reduction of 21% in enteric methane emission in Murrah buffalo calves due to the supplementation of saponin-containing lucerne fodder as 30% of the diet. In an *in vitro* study, Malik et al. [18] observed a significant reduction in methane production due to the supplementation of first cut alfalfa fodder. The addition of saponin or saponin-containing fodder affects methanogenesis primarily through the anti-protozoa action or altering the fermentation pattern and direct inhibition of rumen methanogens [19].

3. GHG emissions from manure management

Livestock manure proved a valuable material that contains required nutrients for plant growth and an excellent soil amendment for improving soil quality and health. Methane is a major greenhouse gas emitted from manure during anaerobic decomposition of the organic matter. Another important greenhouse gas is nitrous oxide, which contrarily emits from aerobic storage of excrement. A pictorial presentation of the possible sources for methane and nitrous oxide emission is provided in **Figure 8**. The thick arrow in **Figure 8** represents the major source for a particular GHG.
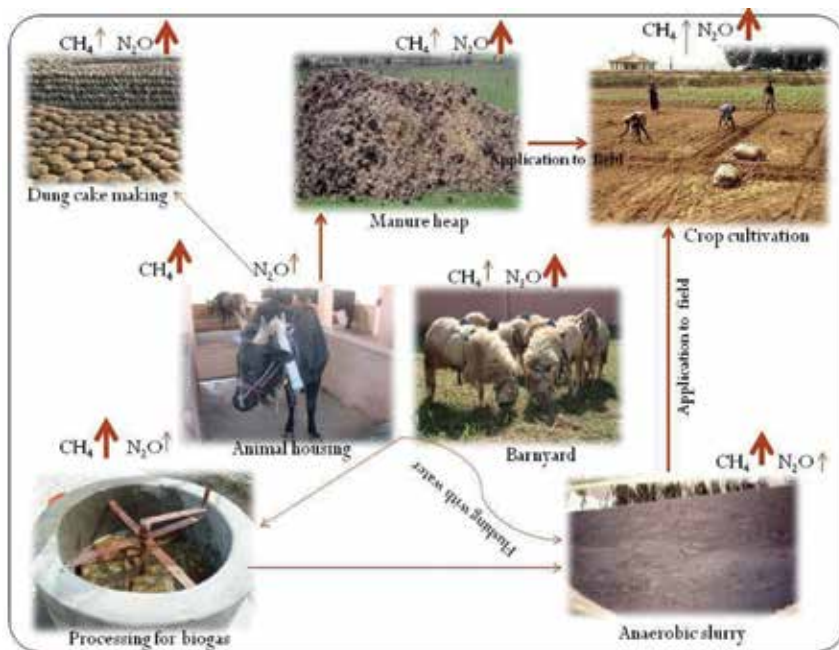
Figure 8. Sources of GHG from livestock excrement.
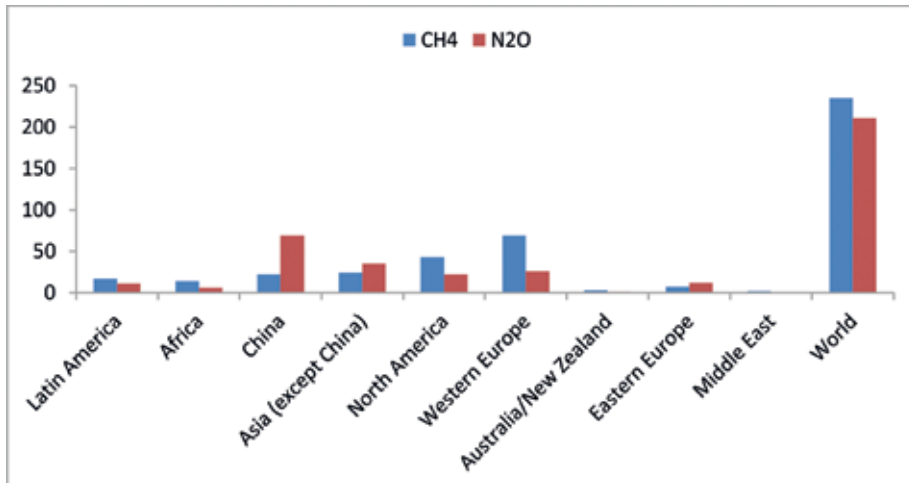
Figure 9. Methane and nitrous oxide emission from manure management in different regions of the world [22] (modified with permission from EPA [3]; O'Mara [21]; UNEP [22]).

The extent of emission of particular greenhouse is determined by the disposal and processing of waste. For example, methane is the primary GHG emit from the excrement, if waste is flushed with water and stored in lagoon; while on the other hand, nitrous oxide is the primary

GHG, if waste is stored as heap in an aerobic environment (**Figure 8**). Methane emission from livestock excrement as such is not a major issue in developing countries, like India. However, excrement is a major source of methane emission in developed world, where excrement is mainly disposed anaerobically. Worldwide production of methane and nitrous oxide annually contribute about 235 and 211 Mt of CO_2 eq, respectively [20, 21]. Regional estimates of manure methane and nitrous oxide are presented in **Figure 9**. Asian countries due to following aerobic storage of excrement contribute about 49% of the total nitrous oxide emissions (**Figure 9**). The aerobic conditions favour nitrous oxide emission from excrement and disfavour methanogenesis. The contribution from America and Africa to total nitrous oxide emission is 15 and 3%, respectively. On the other hand, methane emission from manure is highest in America (22%), which is obviously due to anaerobic processing of animal wastes.

Methane	Manure Methane (kg x 10⁵)		
	Estimated	Projected	
	2010	2025	2050
World	11,414	12,849	15,046
India	1096	1221	1543
% of total	9.6	9.5	10.2
Methane	Manure N₂O (kg x 10⁵)		
	Estimated	Projected	
	2010	2025	2050
World	383	445	516
India	15.3	17.5	21.4
% of total	3.9	3.9	4.1

Table 2. Estimate and projected emissions of methane and methane from manure management [23].

Patra [23] has estimated the methane and nitrous oxide emissions from manure management and also made projections for 2025 and 2050 (**Table 2**). He projected a small increase from 9.6 to 10.2% to the manure methane emission in India over a period of 30 years (**Table 2**). Likewise a small increase is also projected for manure nitrous oxide emission from both world and India. He projected an increase of 133 Mt CO_2 eq nitrous oxide from total manure produced in the world; while in India it would be around 6 Mt CO_2 eq between 2010 and 2030.

The type and quantity of diet are deciding factors for the extent of methane emission from a given volume of manure [24]. International Panel on Climate Change (IPCC) proposed a value of 0.24 L methane per gram of volatile solids (VSs) for dairy cattle [25]. Hashimoto et al. [26] evaluated the methane emission from manure of beef cattle fed different quantities of corn silage and corn grain in the following percentage: 92–0%, 40–53% and 7–88%, respectively. The corresponding emission figures were 0.173, 0.232 and 0.290 L per gram of VS, respectively.

Manure management is an essentiality to be considered for minimizing GHG emissions from excrement processing. The decomposition of dung under anaerobic conditions produces methane. Anaerobic conditions usually arise when dung is mainly disposed along with liquid. Total dung produced and the fraction that undergoes anaerobic decomposition influence methane emissions. When manure is stored or treated as a liquid in lagoons, ponds, tanks or pits, it decomposes anaerobically and produces significant methane. The temperature and the retention in storage vat greatly affect the degree of methanogenesis. Handling dung in the solid form (e.g. stacks or heap) or deposition in pasture and rangelands, accelerate the aerobic decomposition and hence, produce very less methane. The methane production from dung depends on its VS content. VS are organic content of dung which contains both biodegradable and non-biodegradable fractions. VS excretion rates may be retrieved from the literature or determined by conducting experiments. Enhanced characterisation methods can be used for estimating the VS content [Equation 1] . The VS content of dung is considered equivalent to the undigested fraction of the diet, which is consumed but not digested and therefore, excreted as faeces. VS excretion rate may be worked out using the equation of Dong et al. [27]

Volatile solid excretion rates [27],

$$VS = \left[GE\left(1 - \frac{DE\%}{100} \right) + (UE\ GE) \right]\left[\left(\frac{1 - ASH}{18.45} \right) \right]. \tag{1}$$

Using the VS excretion rate, the methane emission factor from dung may be determined as per The equation 2 given below [27]:

$$EF_{(T)} = \left(VS_{(T)}\ 365 \right)\left[B_{o(T)}\ 0.67\,kg\,/\,m^3 \sum_{S,k} \frac{MCF_{S,k}}{100}\ MS_{(T,S,k)} \right]. \tag{2}$$

Nitrous oxide emissions from manure management directly arise from the nitrification and denitrification process. The extent of nitrous oxide emission from manure during storage depends on nitrogen and carbon contents as well as storage duration. Nitrification, that is, oxidation of ammonia nitrogen to nitrate nitrogen, is a necessary step in the generation of nitrous oxide from animal manures. Nitrification occurs when stored dung has sufficient supply of oxygen. During denitrification, which is an anaerobic process, nitrites and nitrates are converted into nitrous oxide and dinitrogen. Direct nitrous oxide emission from manure management may be estimated using following equation:

Direct nitrous oxide emission from manure management [27]:

$$N_2O_{D(mm)} = \left[\sum_S \left[\sum_S \left(N_{(T)}\ Nex_{(T)}\ MS_{(T,S)} \right) \right] EF_{3(S)} \right] \frac{44}{28}. \tag{3}$$

3.1. Measures for reducing GHG

Precautionary or ameliorative measures to ensure less greenhouse gas emission from manure depend on the storage conditions. Due to contradictory environmental conditions required for methane and nitrous oxide emissions, similar mitigating or precautionary measures cannot tackle both the gases at the same time. Therefore, we should fix the priority before attempting the mitigation and process the excrement accordingly. For mitigating methane and nitrous oxide emissions from manure management, few precautionary/ameliorative measures are furnished in **Table 3**.

GHG	Measures
Methane	• Handling of manure in the solid form or deposition on pasture rather than storing it in a liquid based system. However, this may increase nitrous oxide emission.
	• Capturing methane from manure decomposition for producing renewable energy.
	• Avoid adding straw to manure which serve as a substrate for anaerobic bacteria.
	• Application of manure to soil as early as possible to avoid the anaerobic storage of manure which encourages anaerobic decomposition and favour methanogenesis.
	• Application of manure when soil surface is wet should be avoided as it may lead to increase methane emissions.
	• Improve animal's feed conversion efficiency either by feeding quality feeds or by processing to decrease GHG emissions.
	• Cover lagoons with plastic covers or any other means to capture GHGs.
N_2O	• Manure should apply shortly before crop growth for efficient utilization of available nitrogen by crop.
	• Avoid applying manure in winter as it can lead to high emission.
	• Hot and windy weather should be avoided for applying manure because these conditions can increase nitrous oxide emissions.
	• Follow the ideal practices for improving drainage, avoiding soil compaction, increasing soil aeration, and use nitrification inhibitors.
	• Even application of manure around the pasture.
	• Maintain healthy pastures by implementing beneficial management grazing practices to help increase the quality of forages.
	• Include low protein levels and the proper balance of amino acids in the diet to minimize the amount of nitrogen excreted, particularly in urine. Use phase feeding to match diet to growth and development.
	• Storage underground surface with lower temperatures reduces microbial activities.

Table 3. Precautionary/ameliorative measures for reducing GHG emissions from manure management.

4. Summary

Livestock are the major source for anthropogenic GHG emissions as they tend to emit methane from enteric fermentation and manure management and nitrous oxide from manure management. These GHGs as compared to carbon dioxide have very high global warming potential. Apart from accelerating the global warming, enteric methane emission from livestock also carry off substantial fraction of the energy which is supposed to be used by the host animal. A country like India cannot afford this energy loss, as it demands additional feed resources to compensate the loss. The adoption of mitigation options for enteric methane amelioration should be based on the feasibility of intervention(s) in a specific region. Our focus should be on those approaches which may persist in a long run and lead to 20–25% reduction in enteric methane emission. Methane and nitrous oxide emissions from manure management demands different storage conditions. Due to storage conditions (mainly aerobic), the methane emission from manure in the developing countries is not very alarming and hence, our focus should be on reducing nitrous oxide emission from manure management by developing the interventions which at least ensure that nitrous oxide emission has not gone up while trying to mitigate methane emission from manure management.

Author details

Pradeep Kumar Malik[1*], Atul Purushottam Kolte[1], Arindam Dhali[1], Veerasamy Sejian[1], Govindasamy Thirumalaisamy[1], Rajan Gupta[2] and Raghavendra Bhatta[1]

*Address all correspondence to: malikndri@gmail.com

1 ICAR-National Institute of Animal Nutrition and Physiology, Bangalore, India

2 Indian Council of Agricultural Research, New Delhi, India

References

[1] WRI: Climate Analysis Indicators Tool (CAIT), version 9.0. 2011; World Resource Institute, Washington DC, USA

[2] Takahashi J: Perspective on livestock generated GHGs and climate. In: Malik PK, Bhatta R, Takahashi J, Kohn RA and Prasad CS (eds). Livestock production and climate change. CABI book published by CAB International UK and USA; 2015. pp. 111–124.

[3] EPA, Holtkamp J, Hayano D, Irvine A, John G, Munds Dry O, Newland T, Snodgrass S, Williams M: Inventory of U.S. greenhouse gases and sinks: 1996–2006. Environmental

Protection Agency, Washington, DC; 2006, http://www.epa.gov/climatechange/emissions/ downloads/08_Annex_1-7.pdf

[4]   EPA: Global mitigation of non-CO2 greenhouse gases:2010-2013. United States Environmental Protection Agency 2013. Office of Atmospheric Programs (6207J) EPA-430-R-13-011 Washington, DC.

[5]   EPA: Global mitigation of non-CO2 greenhouse gases: 2010–2013. United States Environmental Protection Agency, Washington; 2013, EPA-430-R-13-011.

[6]   Crutzen PJ, Aselmann I, Seiler W: Methane production by domestic animals, wild ruminants, other herbivorous fauna, and humans. Tellus. 1986; 38B: 271–284.

[7]   Van Nevel CJ, Demeyer DI: Control of rumen methanogenesis. Environmental Monitoring and Assessment. 1996; 42: 73–97. DOI: 10.1007/BF00394043.

[8]   19th Livestock Census: All India Report 2012. Ministry of Agriculture, Department of Animal Husbandry, Dairying and Fisheries, Krishi Bhavan, New Delhi. p. 130.

[9]   Bhatta R, Malik PK, Kolte AP, Gupta R: Annual progress report of outreach project on methane. NIANP, Bangalore, India; 2016.

[10] Woese CR, Kandler O, Wheelis ML: Toward a natural system of organisms: proposal for the domains Archaea, Bacteria, and Eucarya. Proceedings of the National Academy of Sciences USA. 1990; 87, 4576–4579.

[11] Hegarty RS, Gerdes R: Hydrogen production and transfer in the rumen. Recent Advances in Animal Nutrition. 1998; 12, 37–44.

[12] Bhatta R, Uyeno Y, Tajima K, Takenaka A, Yabumoto Y, Nonaka I, Enishi O, Kurihara M: Difference in the nature of tannins on *in vitro* ruminal methane and volatile fatty acid production and on methanogenic archaea and protozoal populations. Journal of Dairy Science. 2009; 92: 5512–5522.

[13] Hristov AN, Joonpyo Oh, Lee C, Meinen R, Montes F, Ott T, et al: Mitigation of greenhouse gas emissions in livestock production: a review of technical options for non-CO_2 emissions. In: Gerber P, Henderson B and Makkar H (eds.), FAO Animal Production and Health Paper No. 177, FAO, Rome, Italy; 2013.

[14] Bhatta R, Baruah L, Saravanan M, Suresh KP, Sampath KT: Effect of medicinal and aromatic plants on rumen fermentation, protozoal population and methanogenesis in vitro. Journal of Animal Physiology and Animal Nutrition. 2013; 97: 446-456.

[15] Bhatta R, Saravanan M, Baruah L, Sampath KT, Prasad CS: *in vitro* fermentation profile and methane reduction in ruminal cultures containing secondary plant compounds. Journal of Applied Microbiology. 2013; 115: 455–465.

[16] Malik PK, Singhal KK: Influence of supplementation of wheat straw based total mixed ration with saponins on total gas and methane production in vitro. Indian Journal of Animal Sciences. 2008; 78: 987–990.

[17] Malik PK, Singhal KK: Effect of alfalfa fodder supplementation on enteric methane emission measured by sulfur hexafluoride technique in murrah buffaloes. Buffalo Bulletin. 2016; 35: 125–134.

[18] Malik PK, Singhal KK, Deshpande SB: Effect of lucerne fodder (first cut) supplementation on *in vitro* methane production, fermentation pattern and protozoal counts. Indian Journal of Animal Sciences. 2010; 80: 998–1002.

[19] Malik PK, Bhatta R, Soren NM, Sejian V, Mech A, Prasad KS, Prasad CS: Feed-based approaches in enteric methane amelioration. In: Malik PK, Bhatta R, Takhashi J, Kohn RA and Prasad CS (eds), Livestock production and climate change. CABI Publishers, Oxfordshire, UK; 2015. pp. 336–359.

[20] EPA: Global anthropogenic non-CO2 greenhouse gases emissions: 1990–2020. United States Environmental Protection Agency, , Washington; June 2006, EPA 430-R-06-003

[21] O'Mara FP: The significance of livestock as a contributor to global greenhouse gas emission today and in the near future. Animal Feed Science and Technology. 2011; 166–167: 7–15.

[22] UNEP: Growing greenhouse gas emissions due to meat production. UNEP Global Environmental Alert Service (GEAS); 2012. Available from: http://www.unep.org/pdf/unep-geas_oct_2012.pdf

[23] Patra AK: Trends and projected estimates of GHG emissions from Indian livestock in comparison with GHG emissions from world and developing countries. Asian-Australian Journal of Animal Sciences. 2014; 27: 592–599.

[24] Masse DI, Masse L, Claveau S, Benchaar C, Thomas O: Methane emissions from manure storages. Transactions of the ASABE. 2008; 51: 1775–1781.

[25] IPCC, Watson RT, Zinyowera MC, Moss RH (eds): The regional impacts of climate change: an assessment of vulnerability. Cambridge University Press, Cambridge, UK; 1997. 517 p.

[26] Hashimoto AG, Varel VH, Chen YR: Ultimate methane yield from beef cattle manure: effect of temperature, ration constituents, antibiotics, and manure age. Agricultural Wastes. 1981: 3(4): 241–256.

[27] Dong H, Mangino J, McAllister TA, Hatfield JL, Johnson DE, Lassey KR, de Lima MA, Romanovskya A: Emission from livestock and manure management (Chapter 10). In: 2006 IPCC guidelines for National Greenhouse Gas Inventories, Volume 4: Agriculture, Forestry and Other Land Use; 2006. Available online at http://www.ipcc-nggip.iges.or.jp/public/2006gl/pdf/4_Volume4/V4_10_Ch10_Livestock.pdf

Effect of Dopants on the Properties of Zirconia-Supported Iron Catalysts for Ethylbenzene Dehydrogenation with Carbon Dioxide

Maria do Carmo Rangel, Sirlene B. Lima,
Sarah Maria Santana Borges and
Ivoneide Santana Sobral

Additional information is available at the end of the chapter

Abstract

Due to the harmful effects of carbon dioxide to the environment, a lot of work has been carried out aiming to find new applications, which can decrease the emissions or to capture and use it. An attractive application for carbon dioxide is the synthesis of chemicals, especially for producing styrene by ethylbenzene dehydrogenation, in which it increases the catalyst activity and selectivity. In order to find efficient catalysts for the reaction, the effect of cerium, chromium, aluminum, and lanthanum on the properties of zirconia-supported iron oxides was studied in this work. The modified supports were prepared by precipitation and impregnated with iron nitrate. The obtained catalysts were characterized by thermogravimetry, Fourier transform infrared spectroscopy, X-ray diffraction, specific surface area measurement, and temperature-programmed reduction. The catalysts showed different textural and catalytic properties, which were associated to the different phases in the solids, such as monoclinic or tetragonal zirconia, hematite, maghemite, cubic ceria, monoclinic or hexagonal lantana, and rhombohedral chromia, the active phases in ethylbenzene dehydrogenation. The most promising dopant was cerium, which produces the most active catalyst at the lowest temperature, probably due to its ability of providing lattice oxygen, which activates carbon dioxide and increases the reaction rate.

Keywords: carbon dioxide, styrene, ethylbenzene, dehydrogenation, zirconia, iron oxide

1. Introduction

3 Although greenhouse gas emissions are reaching alarming rates, 80% of the world's energy consumption still comes from fossil fuels, which have been pointed out as the largest source of carbon dioxide emissions [1]. Over the past decade, the global emissions of carbon dioxide from fossil fuels have increased by 2.7% each year and currently are 60% above the levels registered in 1990, which is considered the reference year for the Kyoto Protocol [2]. On the other hand, it is expected that carbon dioxide emissions should reduce by at least 50% to limit the rise of the global average temperature to 2°C by 2050 [3]. Nowadays, the major environmental concerns worldwide, global warming and the acidification of the oceans, are mainly ascribed to the increase of carbon dioxide concentration [4, 5]. Therefore, several alternatives have been proposed to decrease the carbon dioxide concentration and then to mitigate the environment changes. They include demand-side conservation, supply-side efficiency improvement, increasing reliance on nuclear and renewable energy, and carbon capture and storage (CCS) systems [6]. Among them, CCS is considered the most practical approach for long-term carbon dioxide emission reductions, since fossil fuels will continue to be the major source of energy in the next future. However, there are still some technical and economic barriers to be overcome before it can be used on a large scale. One of the main obstacles is the required large capital investment, besides technical difficulties, such as carbon dioxide leakage rates and limited geological storage capacity. Other drawbacks include the costs of transportation and injection when carbon dioxide is only available offshore, such as in United Kingdom, Norway, Singapore, Brazil, and India [7, 8]. Therefore, a more suitable alternative is to capture and use carbon dioxide (carbon capture and utilization [CCU]), changing the waste carbon monoxide emissions into valuable products such as chemicals and fuels, while contributing to climate change mitigation [9].

Captured carbon dioxide can be used as a commercial product, both directly or after conversion. In food and drink industries, for instance, carbon dioxide is often used as a carbonating agent, preservative, packaging gas, and for extracting flavors, as well as in the decaffeination process. In the pharmaceutical industry, it is used as a respiratory stimulant or for the synthesis of drugs. However, these applications are restricted to high-purity carbon dioxide, as that obtained in ammonia plants [9, 10]. Moreover, pressurized carbon dioxide has been investigated for wastewater treatment and water disinfection [11]. Other direct applications of carbon dioxide include enhanced oil recovery and coal-bed methane recovery, where crude oil is extracted from an oil field or natural gas from unminable coal deposits [9].

In the production of chemicals and fuels, carbon dioxide has attracted increasing attention over several decades, for the synthesis of various fine and bulk chemicals. It has already been used in the industrial production of urea, cyclic carbonates, salicylic acid, and methanol [12]. It is expected that carbon dioxide can produce feedstock for chemical, pharmaceutical, and polymer industries by carboxylation reactions to obtain organic compounds, such as carbonates, acrylates, and polymers, or by reduction reactions, where the C=O bonds are broken to produce chemicals such as methane, methanol, syngas, urea, and formic acid [9, 13]. Carbon dioxide can have several other applications, both as carbon or oxygen sources, for the synthesis

of chemicals by several processes, as solvent and/or as reactants. It has potential applications in supercritical conditions, in direct carboxylation reactions, in the conversion of natural gas to liquid (GTL technology), and in methanol synthesis [14]. Carbon dioxide can also act as an oxidant in the dehydrogenation of ethane [15], propane [16], isobutene [17], and ethylbenzene [18–20], as well as in methane dry reforming [21] and oxidative coupling of methane [22]. It is expected that the 115 million metric tons of carbon dioxide, currently consumed every year as feedstock in a variety of synthetic processes, can be triplicated by the use of new technologies [19]. In addition, carbon dioxide can overcome several drawbacks of the processes, especially in the case of dehydrogenation reactions.

In industrial processes, the dehydrogenation of hydrocarbons is often carried out at high temperatures to increase the conversion because of its reversibility and limitation by thermo-dynamic equilibrium. Besides being an energy-consuming process, the high temperatures cause the hydrocarbons cracking, decreasing the selectivity. On the other hand, by the oxidation of the produced hydrogen or by using an oxidant in the presence of a catalyst, these difficulties can be overcome, since the oxidative dehydrogenation is exothermic and can be performed at low temperatures, making negligible the formation of cracking products. Therefore, the use of an oxidant increases the catalyst selectivity and decreases the undesirable products, besides other advantages. Among the oxidizing agents, carbon dioxide has proven to be the most promising one for dehydrogenation reactions [23]. In the ethylbenzene dehy-drogenation, for instance, the use of carbon dioxide can provide a route, which represents an elegant and promising alternative to the conventional process of styrene production.

Currently, the ethylbenzene dehydrogenation in the presence of overheated steam [Eq. (1)] is the main commercial route to produce styrene, one of the most used intermediate for organic synthesis. It is the main building block for several polymers, such as polystyrene, styrene-butadiene rubber, styrene-acrylonitrile, acrylonitrile-butadiene-styrene, and other high-value products. The ethylbenzene dehydrogenation supplies 90% of the global production of styrene, which was around 30×10^6 t in 2010 [24].

$$C_6H_5CH_2CH_{3(g)} + H_2O_{(g)} \longrightarrow C_6H_5CH=CH_{2(g)} + H_{2(g)} \qquad (1)$$
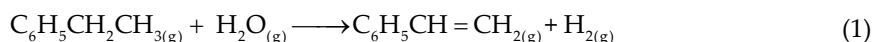
In spite of this fact, the commercial process still has several drawbacks, such as the high consumption of energy, the reaction endothermicity ($\Delta H = 124.85$ kJ/mol), the equilibrium limitation of reaction, and the catalyst deactivation [25]. On the other hand, the replacement of steam by carbon dioxide leads to a consumption of $1.5–1.9 \times 10^8$ cal, instead of 1.5×10^9 cal/mol of styrene produced. In this case, hydrogen is continuously removed as steam by the reverse water gas shift reaction, and the equilibrium is shifted to the formation of dehydro-genation products [Eq. (2)]. In addition, carbon dioxide removes the coke deposits formed during the reaction [26].

$$C_6H_5CH_2CH_{3(g)} + CO_{2(g)} \longrightarrow C_6H_5CH=CH_{2(g)} + CO_{(g)} + H_2O_{(g)} \qquad (2)$$
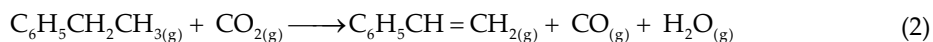
The use of carbon dioxide includes other advantages such as being an inexpensive, nontoxic, and renewable feedstock, which provides a positive impact on the global carbon balance. In addition, it can accelerate the reaction rate, improve styrene selectivity, decrease the thermo-dynamic limitations, suppress the total oxidation, increase the catalyst life, and avoid hotspots [27]. Therefore, the ethylbenzene dehydrogenation with carbon dioxide has been studied over several different catalysts, including iron oxide, vanadium oxide, antimony oxide, chromium oxide, cerium oxide, zirconium oxide, lanthanum oxide, perovskites, and the oxide catalysts promoted with alkali metals supported on several oxides [16, 19, 20, 24, 26–33]. In addition, several works have shown that carbon-based catalysts are active and selective to produce styrene through ethylbenzene dehydrogenation with carbon dioxide. Activated carbons [34, 35], carbon nanofibers [36], onion-like carbons [37], diamonds and nanodiamonds [37, 38], graphites [39], and multiwalled carbon nanotubes (MWCNTs) [40], among others, have been evaluated in ethylbenzene dehydrogenation.

These studies have shown that the effect of carbon dioxide on the activity, selectivity, and stability of the catalysts for ethylbenzene dehydrogenation depends on the kind of the catalyst, as well as on the reaction conditions. For zirconia-based catalysts, the positive effect of carbon dioxide was found to be highly dependent on the crystalline phase at 550°C. It was noted that the tetragonal phase showed high activity and selectivity to styrene, a fact that was related to differences in specific surface area of the solids and their affinity with carbon dioxide associated with the surface basic sites [41, 42]. In a previous work [19], we have found that zirconia was the most active and selective catalyst to produce styrene through ethylbenzene dehydrogen-ation with carbon dioxide, as compared to metal oxides such as lantana (La_2O_3), magnesia (MgO), niobia (Nb_2O_5), and titania (TiO_2). This finding was related to the highest intrinsic activity of zirconia.

In spite of the numerous studies on the catalyst properties for the dehydrogenation of ethylbenzene in the presence of carbon dioxide, no satisfactory catalyst was found yet, requiring new developments. In the present work, the effect of cerium, chromium, aluminum, and lanthanum on the properties of zirconia-supported iron oxides was studied aiming to find efficient catalysts for the reaction.

2. Experimental

2.1. Catalysts preparation

The precursor of zirconium oxide was obtained by hydrolysis of zirconium oxychloride (1 mol/l) with an ammonium hydroxide solution (30% w/v). The obtained gel was rinsed with an ammonium hydroxide solution (1% w/v) eight times up not to detect chloride ions by Mohr's method anymore. The gel was then dried in an oven at 120°C, for 12 h. The solid was calcined at 600°C, for 4 h, under airflow (50 ml/min).

The metal-doped zirconia samples were prepared by the same method, using solutions of zirconium oxychloride and of metal nitrates (Zr/M = 10), where M = Ce (FCEZ sample), Cr

(FCRZ sample), Al (FALZ sample and La (FLAZ sample). Cerium, chromium, aluminum, and lanthanum oxides were also prepared following the same procedure, using aluminum nitrate, cerium nitrate, lanthanum nitrate, and chromium nitrate, respectively, to be used as references.

The modified zirconium oxides were subsequently impregnated with an iron nitrate solution (0.17 mol/l), at room temperature, to obtain the catalysts.

2.2. Catalysts characterization

After iron impregnation, the samples (catalyst precursors) were analyzed by thermogravimetry (TG) and Fourier transform infrared spectroscopy (FTIR).

After calcination, the catalysts were characterized by Fourier transform infrared spectroscopy, X-ray diffraction (XRD), specific surface area measurement, and temperature-programmed reduction.

The experiments of thermogravimetry (TG) were performed on a Mettler Toledo TGA/SDTA 851 equipment. The sample (0.02 g) was placed in a platinum crucible and heated (10°C/min) from room temperature to 1000°C, under airflow (50 ml/min).

The presence of nitrate species in the samples was detected by FTIR, using a Perkin Elmer, Model—Spectrum One, equipment, in the range of 400–4000 cm^{-1}. The samples were prepared as potassium bromide discs, in a 1:10 proportion.

The experiments of X-ray diffraction (XRD) were carried out in a Shimadzu model XD3A apparatus, using CuKα radiation generated at 30 kV and 20 mA and nickel filter.

The specific surface areas were measured in a Micromeritics ASAP 2020, using the sample (0.2 g) previously heated at 300°C, under nitrogen flow.

The curves of temperature-programmed reduction were obtained on a Micromeritics model TPR/TPD 2900 equipment, utilizing 0.3 g of the sample, and heating the solid with a rate of 10°C/min, under flow of a mixture of 5% hydrogen in nitrogen up to 1000°C.

2.3. Catalysts evaluation in ethylbenzene dehydrogenation with carbon dioxide

The catalysts were evaluated in ethylbenzene dehydrogenation in the presence of carbon dioxide in a fixed bed reactor, using 0.3 g of catalyst, at several temperatures (530, 550, 570, 590, 610, and 630°C) under atmospheric pressure. A carbon dioxide to ethylbenzene molar ratio of 10 was used for all experiments.

The reaction products were analyzed by online gas chromatography, using a Varian Star 3600 Cx equipment with a flame ionization detector. A commercial catalyst for the ethylbenzene dehydrogenation with steam, based on iron and chromium oxides, was also evaluated in the same conditions, for comparison.

3. Results and discussion

3.1. Thermogravimetry

The TG curves for the catalyst precursors (before calcination) are displayed in **Figure 1**. For all cases, there was a weight loss in two stages: the first at around 200°C, related to loss of volatiles adsorbed on the solids; the second stage at higher temperatures, in the range of 200–450°C, can be assigned to the decomposition of iron hydroxide to produce hematite and/or maghemite [43, 44]. It can be noted that the kind of the support affected hematite formation, probably due to different interactions of the iron oxide precursor with the support. The process was easier over lanthanum-doped zirconia (225°C), followed by cerium-doped zirconia (250°C). On the other hand, for aluminum-doped zirconia (292°C) and for chromium-doped zirconia (300°C), the process was delayed, suggesting that iron hydroxide was more strongly bonded to these supports.
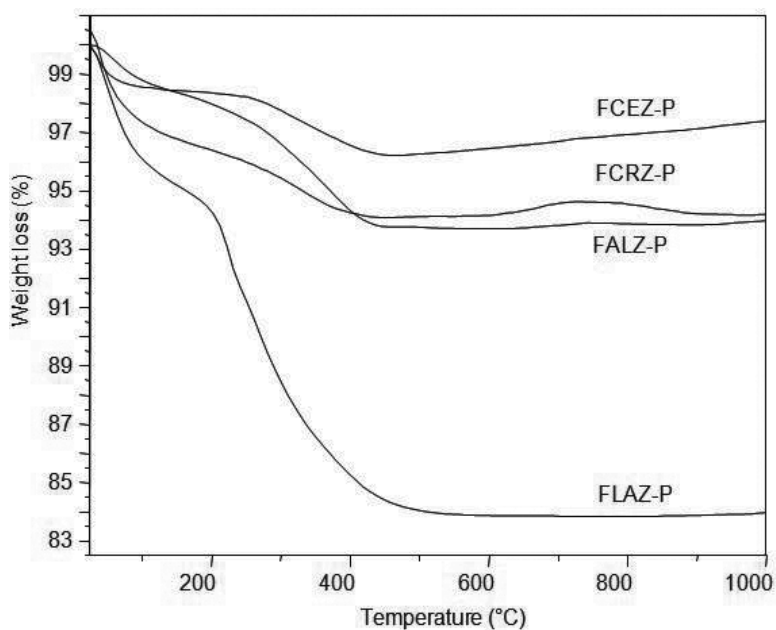
Figure 1. TG curves for the catalyst precursors. F, iron; CE, cerium; CR, chromium; AL, aluminum; LA, lanthanum; Z, zirconia.

3.2. Fourier transform infrared spectroscopy

The FTIR spectra for the precursors (**Figure 2a**) show two bands at 3400 and 1600 cm^{-1}, assigned to the bending vibrations of OH groups in iron hydroxides and in adsorbed water [45]. The absorption at 1384 cm^{-1} is related to the nitrate species [46], from iron nitrate. In the low-frequency region, a broad band was observed, in the range of 800–400 cm^{-1}, attributed to the

Fe–O bond [45]. For the catalysts (**Figure 2b**), it can noted that the band at 1384 cm^{-1} decreased for the samples, except for chromium-doped catalyst, indicating that the calcination was effective for the removal of nitrate species.
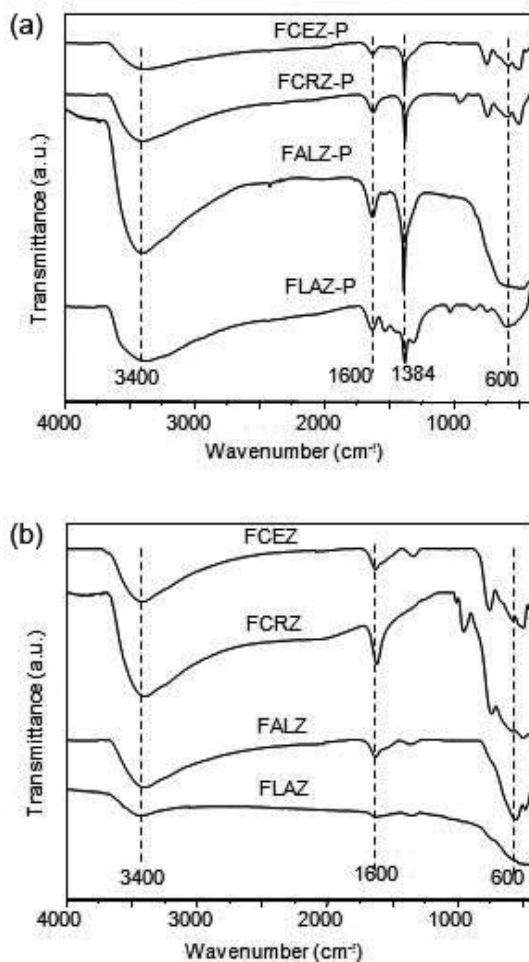
Figure 2. FTIR spectra for the precursors (P) and for the catalysts. F, iron; CE, cerium; CR, chromium; AL, aluminum; LA, lanthanum; Z, zirconia.

3.3. X-ray diffraction

From the X-ray diffractograms of the solids (**Figure 3**), different phases were found for all samples, related to the different oxides. However, for most cases, it was not possible to assure the presence of isolated phases of iron, zirconium, and of the dopants. Therefore, hematite, α-Fe_2O_3 (JCPDS 871166), maghemite, γ-Fe_2O_3 (JCPDS 251402), or zirconium oxide, ZrO_2 (monoclinic, JCPDS 830944 and tetragonal, JCPDS 881007), as well as lanthanum oxide, La_2O_3

(monoclinic, JCPDS 220641 or hexagonal, JCPDS 401279), aluminum oxide, Al_2O_3 (orthorhombic, JCPDS 880107), or chromium oxide, Cr_2O_3 (rhombohedral, JCPDS 841616), cannot be detected, because of the coincidence of the diffraction peaks of these phases. Only maghemite and the cubic phase of ceria, CeO_2 (JCPDS 780694), were detected as isolated phases for the chromium and cerium-doped samples, respectively.
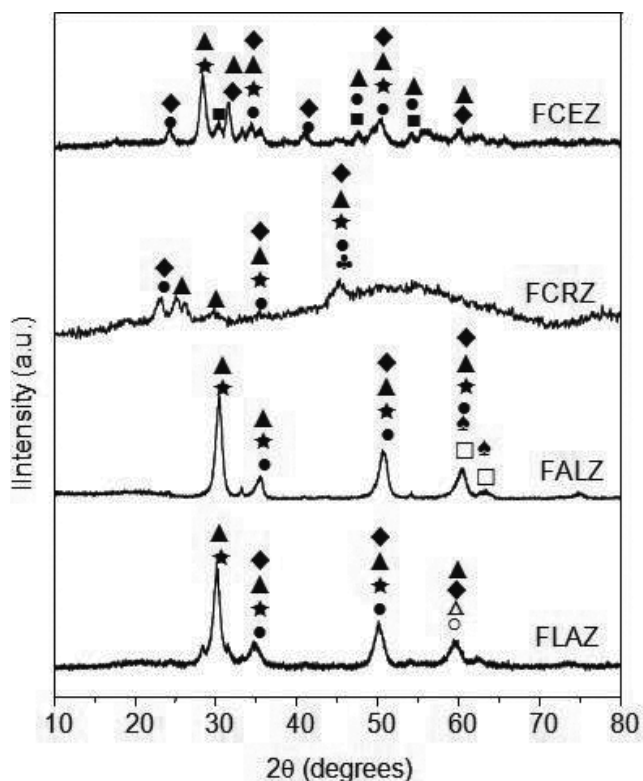
Figure 3. X-ray diffractograms for the catalysts. F, iron; CE, cerium; CR, chromium; AL, aluminum; LA, lanthanum; Z, zirconia. ♦: hematite (α-Fe_2O_3), ematite (ray dγ-Fe_2O_3, ★: tetragonal zirconia (ZrO_2), ●, monoclinic zirconia (ZrO_2), ■, cubic ceria (CeO_2), ♣: rhombohedral chromia (Cr_2O_3), Δ:hexagonal lantana (La_2O_3), ○, monoclinic lantana (La_2O_3), □: orthorhombic alumina (Al_2O_3), ♠: monoclinic alumina (Al_2O_3).

3.4. Specific surface areas

Table 1 shows the specific surface areas of the catalysts, as well as of pure and doped supports. It can be noted that pure oxides showed different values, which are typical of the nature of each oxide. Zirconia showed the highest values, while chromium showed the lowest one. In addition, the dopants changed the specific surface area of zirconia (73 m^2/g), depending on the kind of dopant. These different behaviors are related to the size of the ions, the possibility of the ion to enter into zirconia lattice, and the formation of mixed compounds. According to previous studies [47–49], it would be expected that these dopants would in-

crease the specific surface areas of zirconia, because of the differences in ionic radius of cerium (0.97 Å), chromium (0.615 Å), aluminum (0.54 Å), and lanthanum (1.16 Å), as compared to zirconium (0.84 Å). These differences often cause stresses in zirconia lattice, favoring the production of smaller particles, since they decrease the stress to surface ratio. However, only for the aluminum-doped zirconia the specific surface area increased, suggesting that most of the dopants did not enter into the lattice but rather remain as a segregated phase, as detected for cerium-doped zirconia.

The impregnation of iron on the supports also changes the specific surface areas, as shown in **Table 1**. For the chromium-doped and lanthanum-doped samples, the addition of iron caused an increase in specific surface area, suggesting a contribution of the iron oxides to these values. On the other hand, the other samples showed a decrease in the specific surface area, indicating that they went on sintering during the calcination step, after iron impregnation. The chromium-based catalyst showed the highest value, while the cerium-based catalyst showed the lowest one.

Samples	Sg (m^2/g)
Z	73
CE	38
CR	1.7
AL	23
LA	17
CEZ	74
CRZ	17
ALZ	98
LAZ	19
FCEZ	58
FCRZ	127
FALZ	85
FLAZ	95

Z, zirconia; CE, cerium or ceria; CR, chromium or chromia; AL, aluminum or alumina; LA, lanthanum or lanthana; F, iron oxide.

Table 1. Specific surface areas (Sg) of pure oxides, doped zirconia, and of iron oxide supported on doped zirconia.

3.5. Temperature-programmed reduction

The catalysts showed different reduction profiles, as displayed in **Figure 4**. The cerium-doped catalyst showed a peak beginning at 192°C and others in the range from 398 to 931°C. The first peak can be assigned to the reduction of Fe^{+3} to Fe^{+2} species, while the latter is due to the reduction of Fe^{+2} to Fe^0 species [50], as well as to the reduction processes related to the support

[32, 33]. On the other hand, the chromium-doped zirconia sample showed a reduction peak beginning at 182°C, with a shoulder at around 274°C, as well as another peak in the range 501–929°C. The first peak can be associated to the reduction of Cr^{+6} to Cr^{+3} [16] species and of Fe^{+3} to Fe^{+2} species, while the latter one is due to the reduction of Fe^{+2} to species Fe^0 [50]. The lanthanum-doped sample showed a peak beginning at 225°C and other ones at 327, 393, and 500°C, attributed to the reduction of Fe^{+3} species in different interactions with the support. A broad peak in the range of 600–781°C is related to the reduction of Fe^{+2} to Fe^0 species and to the processes related to the support. For the aluminum-doped sample, two reduction peaks beginning at 200 and 332°C were noted associated to the reduction of Fe^{+3} to Fe^{+2} species in different interactions with the support. A broad peak in the range of 406–704°C can be assigned to the reduction of Fe^{+2} to Fe^0 species. The easiness of the reduction decreased with the dopants in the order: Cr > Ce > Al > La.
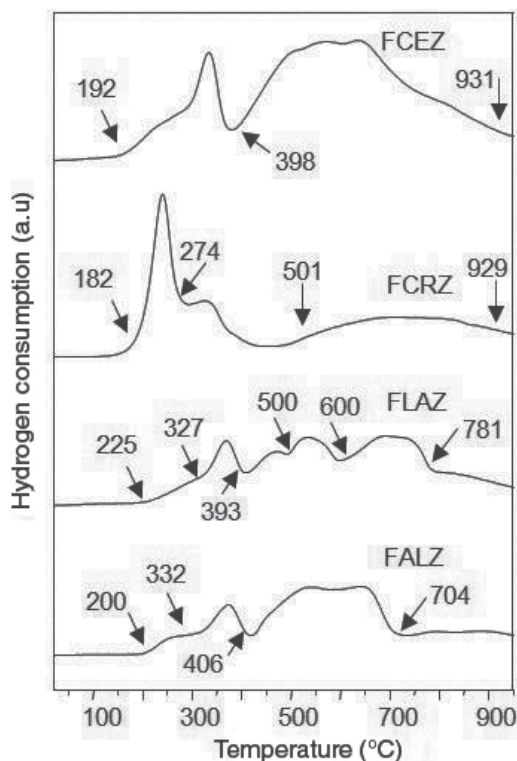
Figure 4. Curves of temperature-programmed reduction for the catalysts. F, iron; CE, cerium; CR, chromium; AL, aluminum; LA, lanthanum; Z, zirconia.

3.6. Activity and selectivity of the catalysts

Figure 5 shows the values of ethylbenzene conversions as a function of temperature during the dehydrogenation with carbon dioxide. It can be noted that the samples were more active

than a commercial catalyst, for all temperature ranges. Also, the catalysts showed different performances, depending on the reaction temperature. At low temperatures, the cerium-based sample led to the highest conversion that, however, decreased with the temperature increase. This can be related to the ability of cerium oxide (detected by X-ray diffraction) for providing lattice oxygen, which activates the carbon dioxide molecule and then increases the reaction rate [32, 33]. The chromium-doped catalyst was the second most active one, leading to conversions of around 46%, which increased with temperature, a fact that can be associated to the high dehydrogenation activity of chromium compounds [16]. The aluminum-doped and lanthanum-doped samples showed similar behaviors, leading to low conversions that increased with temperature.
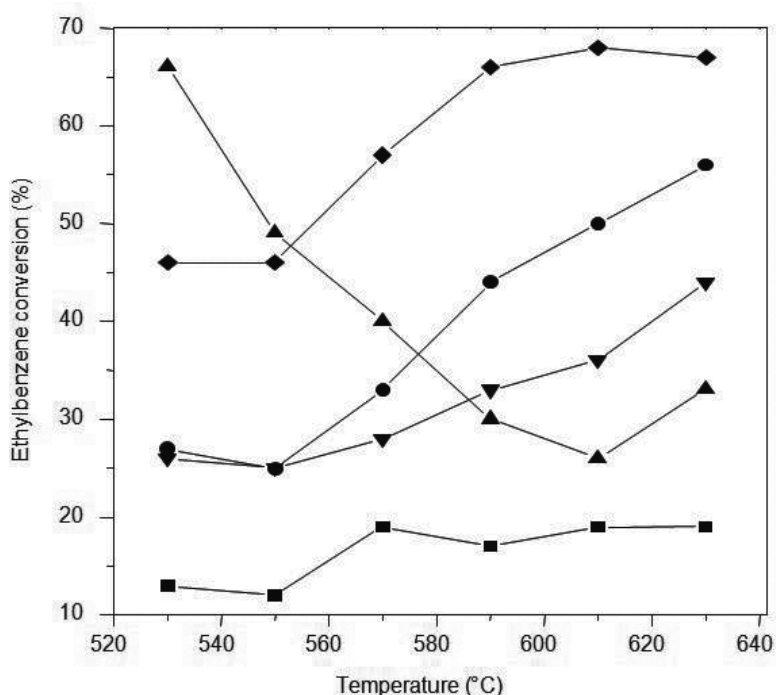
Figure 5. Ethylbenzene conversion over the obtained catalysts and over a commercial catalyst. F, iron; CE, cerium; CR, chromium; AL, aluminum; LA, lanthanum; Z, zirconia.

The selectivity of the catalysts to styrene (**Figure 6**) also changed with the kind of the dopant and with temperature. The aluminum-doped catalyst was the most selective one, but the selectivity decreased as the temperature increased. A similar behavior was noted for the commercial catalyst. On the other hand, the selectivity of cerium-doped sample showed a maximum at around 570°C, while the selectivity of lanthanum-based and chromium-based solids almost did not change with temperature. These findings can be related to the kind of the dopants and their different interactions with the support, as well as to the reaction temperature.
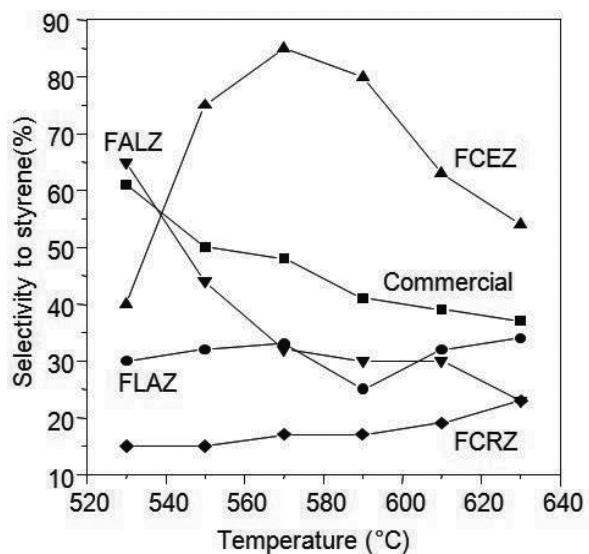
Figure 6. Selectivity to styrene of the obtained catalysts and of a commercial catalyst, during ethylbenzene conversion. F, iron; CE, cerium; CR, chromium; AL, aluminum; LA, lanthanum; Z, zirconia.
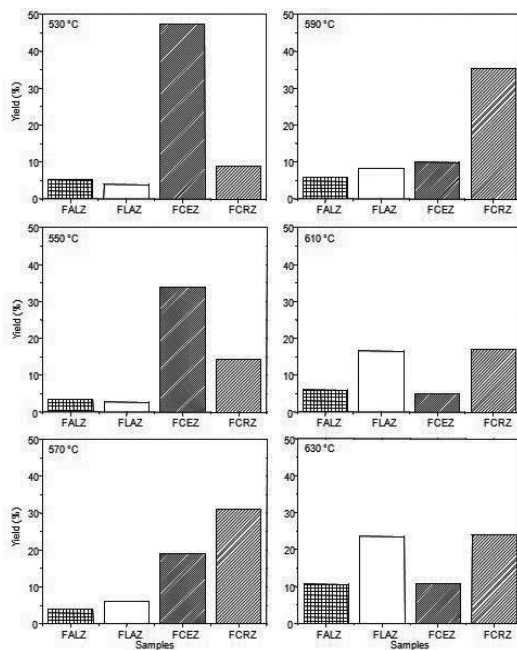
Figure 7. Styrene yields over the obtained catalysts and over a commercial catalyst, during ethylbenzene conversion. F, iron; CE, cerium; CR, chromium; AL, aluminum; LA, lanthanum; Z, zirconia.

Figure 7 shows the yields obtained over the catalysts. One can see that the yield largely depends on the reaction temperature and on the kind of the dopant. The highest value was obtained at 530 and 560°C, over the cerium-doped catalyst. However, the yield decreased with temperature increase, suggesting the catalyst deactivation at high temperatures. While the other catalysts showed low yields for all temperature ranges, the chromium-doped catalyst led to a yield of around 35% at 590°C.

4. Conclusions

Catalysts based on iron oxides (hematite and/or maghemite), supported on zirconium oxide doped with cerium, chromium, aluminum, or lanthanum, show different textural and catalytic properties in ethylbenzene dehydrogenation with carbon dioxide. These findings can be related to the different phases of the supports, such as zirconia (monoclinic or tetragonal), iron oxides (hematite or maghemite), cerium oxide (cubic), lantana (monoclinic or hexagonal), and chromium oxide (rhombohedral), which are also active in the reaction.

The most promising sample was the cerium-doped solid, which led the highest yield (46%) at the lowest temperature. This was assigned to the role of cerium oxide in providing lattice oxygen, which activates carbon dioxide and increases the reaction rate.

The catalysts have proven to provide another alternative to use carbon dioxide, one of the main greenhouse gas and then to contribute to the environment protection.

Acknowledgements

Author details

Maria do Carmo Rangel[1,2*], Sirlene B. Lima[1,2], Sarah Maria Santana Borges[1] and Ivoneide Santana Sobral[1]

*Address all correspondence to: mcarmov@ufba.br

1 Grupo de Estudos em Cinética e Catálise, Instituto de Química, Universidade Federal da Bahia, Campus Universitário de Ondina, Salvador, Bahia, Brazil

2 Programa de Pós-Graduação em Engenharia Química, Rua Aristides Novis, Salvador, Bahia, Brazil

References

[1]   Abass AO. Valorization of greenhouse carbon dioxide emissions into value-added products by catalytic processes. Journal of CO_2 Utilization. 2013;3-4:74–92. DOI: 10.1016/j.jcou.2013.10.004

[2]   Quéré CL, Peters GP, Andres RJ, Andrew RM, Boden T, Ciais P, Friedlingstein P, et al. Global carbon budget. Earth System Science Data Discussion. 2013;6:689–760. DOI: 10.5194/essdd-6-689-2013

[3]   IPCC, Climate Change 2013: The Physical Science Basis, Intergovernmental Panelon Climate Change [Internet]. 2013. Available at: https://www.ipcc.ch/report/ar5/wg1/ [Accessed: 2016-02-11].

[4]   Honisch B, Ridgwell A, Schmidt DN, Thomas E, Gibbs SJ, Sluijs A, Zeebe R, Kump L, Martindale RC, et al. The geological record of ocean acidification. Science. 2012;335:1058–1063. DOI: 10.1126/science.1208277

[5]   Crowley TJ, Berner RA. Enhanced: CO2 and climate change. Science. 2001;292:870–872. DOI: 10.1126/science.1061664

[6]   Spigarelli BP, Kawatra SK. Opportunities and challenges in carbon dioxide capture. Journal of CO2 Utilization. 2013;1:69–87. DOI: 10.1016/j.jcou.2013.03.002

[7]   Ciferno JP, Fout TE, Jones AP, Murphy JT. Capturing carbon from existing coal fired power plants. Chemical Engineering Progress. 2009;105:33–41. ISSN: 03607275

[8]   D'Alessandro DM, Smit B, Long JR. Carbon dioxide capture: Prospects for new materials. Angewandte Chemie International Edition. 2010;49:6058–6082. DOI: 10.1002/anie.201000431

[9]   Cuéllar-Franca RM, Azapagic A. Carbon capture, storage and utilisation technologies: A critical analysis and comparison of their life cycle environmental impacts. Journal of CO2 Utilization. 2015;9:82–102, DOI: 10.1016/j.jcou.2014.12.001

[10] Markewitz P, Kuckshinrichs W, Leitner W, Linssen J, Zapp P, Bongartz R, Schreiber A, Müller TE. Worldwide innovations in the development of carbon capture technologies and the utilization of CO_2. Energy and Environmental Science. 2012;5:7281–7305. DOI: 10.1039/C2EE03403D

[11] Vo HT, Imai T, Ho TT, Dang T-L, Hoang SA. Potential application of high pressure carbon dioxide in treated wastewater and water disinfection: Recent overview and further trends. Journal of Environmental Sciences. 2015;36:38–47. DOI: 10.1016/j.jes.2015.04.006

[12] Plasseraud L. Carbon Dioxide as Chemical Feedstock. In: Aresta, M, editor. Chem Sus Chem; 2010. p. 631–632. DOI: 10.1002/cssc.201000097

[13] Boxun H, Curtis G, Steven LS. Thermal, electrochemical, and photochemical conversion of CO_2 to fuels and value-added products. Journal of CO2 Utilization. 2013;1:18–27. DOI: 10.1016/j.jcou.2013.03.004

[14] Aresta M, Dibenedetto A. Product review. The contribution of the utilization option to reducing the CO_2 atmospheric loading: Research needed to overcome existing barriers for a full exploitation of the potential of the CO_2 use. Catalysis Today. 2004;98:455–462. DOI: 10.1016/j.cattod.2004.09.001

[15] Nakagawa K, Okamura M, Ikenaga N, Suzuki T, Kobayashi T. Dehydrogenation of ethane over gallium oxide in the presence of carbon dioxide. Chemical Communications. 1998;9:1025–1026. DOI: 10.1039/A800184G

[16] Wang S, Murata K, Hayakawa T, Hamakawa S, Suzuki K. Dehydrogenation of ethane with carbon dioxide over supported chromium oxide catalysts. Applied Catalysis A. 2000;196:1–8. ISSN: 0926-860X. DOI:10.1016/S0926-860X(99)00450-0

[17] Shimada H, Akazawa T, Ikenaga N, Suzuki T. Dehydrogenation of isobutane to isobutene with iron-loaded activated carbon catalyst. Applied Catalysis A. 1998;168:243–250. ISSN: 0926-860X. DOI:10.1016/S0926-860X(97)00350-5

[18] Mimura N, Takahara I, Saitoa M, Hattorib T, Ohkumac K, Andod M. Dehydrogenation of ethylbenzene over iron oxide-based catalyst in the presence of carbon dioxide. Catalysis Today. 1998;45:61–64. DOI:10.1016/S0920-5861(98)00246-6

[19] Rangel MC, Monteiro AM, Oportus M, Reyes P, Ramos MS, Lima SB. Ethylbenzene dehydrogenation in the presence of carbon dioxide over metal oxides. In: Guoxiang, L, editor. Greenhouse Gases: Capturing, Utilization and Reduction. Publishing Intech; 2012. p. 117–136. ISBN: 978953-51-0192-5

[20] Rangel MC, Monteiro APM, Marchetti SG, Lima SB, Ramos MS. Ethylbenzene dehydrogenation in the presence of carbon dioxide over magnesia-supported iron oxides. Journal of Molecular Catalysis A, Chemical. 2014;387:147–155. DOI:10.1016/j.molcata.2014.03.002

[21] Rangel MC, de Araújo GC, de Lima SM, Assaf JM, Peña MA, Fierro JLG. Catalytic evaluation of perovskite-type oxide $LaNi_{1-x}Ru_xO_3$ in methane dry reforming. Catalysis Today. 2008;133-135:129–135. DOI:10.1016/j.cattod.2007.12.049

[22] Nishiyama T, Aika K. Mechanism of the oxidative coupling of methane using CO_2 as an oxidant over PbO-MgO. Journal of Catalysis. 1990;122:346–351. DOI:10.1016/0021-9517(90)90288-U

[23] Corberán VC. Novel approaches for the improvement of selectivity in the oxidative activation of light alkanes. Catalysis Today. 2005;99:33–41. DOI:10.1016/j.cattod.2004.09.055

[24] Betiha MA, Rabie AM, Elfadly AM, Yehia FZ. Microwave assisted synthesis of a VOx-modified disordered mesoporous silica for ethylbenzene dehydrogenation in pres-

ence of CO_2. Microporous and Mesoporous Materials. 2016;222:44–54. DOI: 10.1016/j.micromeso.2015.10.009

[25] Nederlof C, Kapteijn F, Makkee M. Catalysed ethylbenzene dehydrogenation in CO_2 or N_2-Carbon deposits as the active phase. Applied Catalysis A. 2012;417-418:163–173. DOI:10.1016/j.apcata.2011.12.037

[26] Mamedov EA, Corberan VC. Oxidative dehydrogenation of lower alkanes on vanadium oxide-based catalysts. The present state of the art and outlooks. Applied Catalysis A. 1995;127:1–40. DOI:10.1016/0926-860X(95)00056-9

[27] Sakurai Y, Suzaki T, Nakagawa K, Ikenagaa N-O, Aota H, Suzuki T. Dehydrogenation of ethylbenzene over vanadium oxide-loaded mgo catalyst: Promoting effect of carbon dioxide. Journal of Catalysis. 2002;209:16–24. Doi:10.1006/jcat.2002.3593

[28] Hong D, Vislovskiy VP, Hwang YK, Hung SHJ, Chang J. Dehydrogenation of ethylbenzene with carbon dioxide over MgO-modified Al2O3-supported V-Sb oxide catalysts. Catalysis Today. 2008;131:140–145. DOI:10.1016/j.cattod.2007.10.020

[29] Burri A, Jiang N, Yahyaoui K, Park S-E. Ethylbenzene to styrene over alkali doped TiO2-ZrO_2 with CO_2 as soft oxidant. Applied Catalysis A: General. 2015;495:192–199. DOI: 10.1016/j.apcata.2015.02.003

[30] Zhang S-J, Li W-Y, Li X-H. Effect of preparation methods on the catalytic properties of Fe_2O_3/Al_2O_3-ZrO_2 for ethylbenzene dehydrogenation. Journal of Fuel Chemistry and Technology. 2015;43:437–441. DOI:10.1016/S1872-5813(15)30012-8

[31] Watanabe R, Saito Y, Fukuhara C. Enhancement of ethylbenzene dehydrogenation of perovskite-type $BaZrO_3$ catalyst by a small amount of Fe substitution in the B-site. Journal of Molecular Catalysis A: Chemical. 2015;404-405:57–64. DOI: 10.1016/j.molcata.2015.04.010

[32] Kovacevic M, Agarwal S, Mojet BL, Ommen JGV, Lefferts L. The effects of morphology of cerium oxide catalysts for dehydrogenation of ethylbenzene to styrene. Applied Catalysis A: General. 2015;505:354–364. DOI: 10.1016/j.apcata.2015.07.025

[33] Li X, Feng J, Fan H, Wang Q, Li W. The dehydrogenation of ethylbenzene with CO_2 over $Ce_xZr_{1-x}O_2$ solid solutions. Catalysis Communications. 2015;59:104–107. DOI: 10.1016/j.catcom.2014.10.003

[34] Zarubina V, Talebi H, Nederlof C, Kapteijn F, Makkee M, Cabrera IM. On the stability of conventionaland nano-structured carbon-based catalystsin theoxidative dehydrogenation of ethylbenzeneunder industrially relevant conditions. Carbon. 2014;77:329–340. DOI: 10.1016/j.carbon.2014.05.036

[35] Oliveira SB, Barbosa DP, Monteiro APM, Rabelo D, Rangel MC. Evaluation of copper supported on polymeric spherical activated carbon in the ethylbenzene dehydrogenation. Catalysis Today. 2008;133-135:92–98. ISSN: 09205861. DOI:10.1016/j.cattod.2007.12.040

[36] Delgado JJ, Chen XW, Frank B, Su DS, Schlögl R. Activation processes of highly ordered carbon nanofibers in the oxidative dehydrogenation of ethylbenzene. Catalysis Today. 2012;186:93–98. DOI:10.1016/j.cattod.2011.10.023

[37] Su D, Maksimova NI, Mestl G, Kuznetsov VL, Keller V, Schlögl R, et al. Oxidative dehydrogenation of ethylbenzene to styrene over ultra-dispersed diamond and onion-like carbon. Carbon. 2007;45:2145–2151. DOI: 10.1016/j.carbon. 2007.07.005

[38] Ba H, Liu Y, Mu X, Doh W-H, Nhut J-M, Granger P, Pham-Huu C. Macroscopic nanodiamonds/β-SiC composite as metal-free catalysts for steam-free dehydro‐ genation of ethylbenzene to styrene. Applied Catalysis A: General. 2015;499:217– 226. DOI: 10.1016/j.apcata.2015.04.022

[39] Li P, Li T, Zhou JH, Sui ZJ, Dai YC, Yuan WK, et al. Synthesis of carbon nanofiber/ graphite-felt composite as a catalyst. Microporous Mesoporous Materials. 2006;95:1–7. DOI:10.1016/j.micromeso.2006.04.014

[40] Qui N, Scholz P, Keller T, Pollok K, Ondruschka B. Ozonated multiwalled carbon nanotubes as highly active and selective catalyst in the oxidative dehydrogenation of ethyl benzene to styrene. Chemical Engineering & Technology. 2013;36:300–306. DOI: 10.1002/ceat.201200354

[41] Vislovskiy VP, Chang J-S, Park M-S, Park S-E. Ethylbenzene into styrene with carbon dioxide over modified vanadia–alumina catalysts. Catalysis Communications. 2002;3:227–231. ISSN: 1566-7367. DOI:10.1016/S1566-7367(02)00105-X

[42] Sun A, Qin Z, Wang J. Reaction coupling of ethylbenzene dehydrogenation with water- gas shift. Applied Catalysis A. 2002;234:179–189. ISSN: 0926-860X. DOI:10.1016/S0926- 860X(02)00222-3

[43] Gadalla AM, Livingston TW. Thermal behavior of oxides and hydroxides of iron and nickel. Thermochimica Acta. 1989;145:l–9. DOI:10.1016/0040-6031(89)85121-4

[44] Silva CLS, Marchetti SG, Faro ACJ, Silva TF, Assaf JM, Rangel MC. Effect of gadolinium on the catalytic properties of iron oxides for WGSR. Catalysis Today. 2013;213:127–134. DOI:10.1016/j.cattod.2013.02.025

[45] Pedrosa J, Costa BFO, Portugal A, Durães L. Controlled phase formation of nanocrystalline iron oxides/hydroxides in solution: An insight on the phase transformation mechanisms. Materials Chemistry and Physics. 2015;163:88–98. DOI:10.1016/j.matchemphys.2015.07.018

[46] Martino AD, Iorio M, Prenzler PD, Ryan D, Obied HK, Arienzo M. Adsorption of phenols from olive oil waste waters on layered double hydroxide, hydrox‐ yaluminium–iron-co-precipitate   and   hydroxyaluminium–iron–montmorillonite complex. Applied Clay Science. 2013;80-81:154–161. DOI:10.1016/j.clay.2013.01.014

[47] Tsipas SA. Effect of dopants on the phase stability of zirconia-based plasma sprayed thermal barrier coatings. Journal of the European Ceramic Society. 2010;30:61–72. DOI: 10.1016/j.jeurceramsoc.2009.08.008

[48] Wiwattanapongpan J, Mekasuwandumrong O, Chaisuk C, Praserthdam P. Effect of dopants on the properties of metal-doped zirconia prepared by the glycothermal method. Ceramics International. 2007;33:1469–1473. DOI: 10.1016/j.ceramint. 2006.05.014

[49] Trunschke A, Hoang DL, Radnik J, Lieske H. Influence of lanthana on the nature of surface chromium species in la2o3-modified crox/zro$_2$ catalysts. Journal of Catalysis. 2000;191:456–466. DOI:10.1006/jcat.1999.2791

[50] Ramos MS, Santos MS, Gomes LP, Albornoz A, Rangel MC. The influence of dopants on the catalytic activity of hematite in the ethylbenzene dehydrogenation. Applied Catalysis A. 2008;341:12–17. DOI:10.1016/j.apcata.2007.12.035

A Comparative Study of Human Health Impacts Due to Heavy Metal Emissions from a Conventional Lignite Coal-Fired Electricity Generation Station, with Post-Combustion, and Oxy-Fuel Combustion Capture Technologies

Jarotwan Koiwanit , Anastassia Manuilova ,
Christine Chan , Malcolm Wilson and
Paitoon Tontiwachwuthikul

Additional information is available at the end of the chapter

Abstract

Carbon dioxide capture has become an important component for ensuring reduction of greenhouse gases in the atmosphere. Even though emission reduction technologies such as electrostatic precipitators (ESP) and flue gas desulfurization (FGD) are in place at most electricity-generating stations today, the large point source emitters of carbon dioxide (CO_2) and other emissions, such as heavy metals, to the atmosphere are still fossil fuel electricity-generating stations. When CO_2 capture is employed, these emissions can be further reduced. However, despite its important ability to reduce atmospheric emissions, the CO_2 capture technology in fact still releases some emissions through its stacks into the air. Since the safety and stability of the CO_2 capture technology are fundamental considerations for widespread social acceptance, the potential liability associated with the capture technology is cited as an important barrier to successful CO_2 capture implementation. Liability of the technology is further clouded by a failure to clearly define what is at risk, especially regarding human health and safety. This research study will focus on investigating the risks associated with human health and safety resulting from the different versions of the technology including: (i) no capture system, (ii) post-combustion, and (iii) oxy-fuel combustion CO_2 capture technology at the Boundary Dam Power Station (BDPS) in Estevan, Saskatchewan, Canada. The research objective of this study was to evaluate the risk to human health associated with the BDPS in Estevan, Saskatchewan, Canada, using the American Meteorological Society's Environmental Protection Agency Regulatory Model (AERMOD) and cancer

and non-cancer risk equations. This research presents the air dispersion modeling of the conventional lignite-fired electricity generation station at the BDPS, the inclusion of post-combustion CO_2 capture technology, and the oxy-fuel carbon dioxide capture process. The heavy metals were measured near the power plant located in Estevan, Saskatchewan. This study shows that the emissions from the three stacks posed cancer risks of less than one chance in a million (1×10^{-6}). There were only two emissions from the "no capture" scenario that caused inhalation cancer risks of more than 1×10^{-6}. In terms of non-cancer risks, the pollutant's concentration from the three stacks was unlikely to cause any non-cancer health effects.

Keywords: carbon dioxide capture, AERMOD, air dispersion, risk, human health

1. Introduction

According to [1], in recent decades, climate change has had the strongest and most comprehensive impact to natural systems [2, 3]. Recent changes in climate affect heat waves, floods, wildfires, ecosystems and human systems. Emissions of CO_2 are known to contribute to the climate change as well. CO_2, a major greenhouse gas (GHG) which results in climate change, is mostly generated from electrical generation that uses fossil fuels (e.g., oil, coal, and natural gas, which are regarded as the world's primary source of energy). To cope with this problem, the use of an effective CO_2 capture technology has become an important approach in ensuring the reduction CO_2 emissions. However, since additional energy is required in carbon capture systems operation, the consumption of primary materials and fuel is increased when compared to the amount used in fossil-fuel-based energy production systems without the carbon capture technology. Consequently, it is necessary to evaluate both the energy utilization of the technology and the risks of the gaseous emissions to human health. This study focuses on the latter consideration.

The objective of this study was to analyze and compare the risks to human health posed by a lignite coal-fired electricity generation station that has the following: (i) no capture system, (ii) post-combustion, and (iii) oxy-fuel combustion CO_2 capture technology at the Boundary Dam Power Station (BDPS) in Estevan, Saskatchewan, Canada. The total area in Estevan is 795.32 square kilometers with a population density of 16.3 persons per square kilometer [4]. For the post-combustion system presented in this paper, the CO_2 is absorbed by a monoethanolamine (MEA) solvent and is purified and compressed for transportation and storage. The fuel in an oxy-fuel technology is combusted in pure oxygen (O_2) (>95% volume), which results in a concentration of CO_2 that is ready for transportation and storage. However, despite its advantages in cutting greenhouse gas (GHG) emissions, post-combustion and the oxy-fuel capture processes also emit some gases through their stacks.

A comparison of the risks to human health posed by a lignite coal-fired electricity generation station that has the following: (i) no capture system, (ii) post-combustion, and (iii) oxy-fuel combustion CO_2 capture technology at the Boundary Dam Power Station (BDPS) in Estevan, Saskatchewan, Canada, will reveal whether there are health-related risks associated

with the different types of carbon capture technology. Understanding the associated risks of the technology can support formulation of the standards and regulatory frameworks required for large-scale application of the carbon capture technology [5]. In this study, the health-related risks of the three technologies are analyzed so as to shed light on the relationships between quantitative emission releases and the probability of occurrences of health effects.

This paper is organized as follows: Section 2 presents some background to the study and provides a discussion on health effects of selected power plant pollutants, Section 3 presents methods of LCA, Section 4 provides several methods for air dispersion modeling and risk assessment of post- and oxy-fuel combustion CO_2 capture processes, Section 5 discusses the results from the analysis, Section 6 gives the discussion, and Section 7 presents conclusion and discusses some direction for future work.

2. Background health effects from typical power plants

2.1. Background and related work

To assess the emissions from the stack and the environmental impacts of the carbon capture technology, three case scenarios of a typical power plant were evaluated. The three scenarios include a power plant with the following: (i) no carbon capture system, (ii) the post-combustion carbon capture system, and (iii) the oxy-fuel combustion carbon capture system. The life cycle inventory (LCI) results generated from a life cycle assessment (LCA) study were used for calculating the pollution concentrations in each grid block within the plume area [6–8]. Air dispersion modeling has been used to evaluate the concentration in each grid block. After that, the concentrations are evaluated for the possible impacts on human health. The emissions released from the tall stacks of the electricity generation plants were not deposited near the source, but further away [9, 10]. $PM_{2.5}$ is ingested into the body via the respiratory system. Hg^0 has the longest atmospheric life span of the various species of mercury and can be transported easily over long distances due to its insolubility in and low reactivity to water. Hg^0 is the common mercury species in lignite [11]. Hg^p and Hg^{2+}, with their high reactivity and solubility in water, can be controlled by some emission control units such as electrostatic precipitators (ESP) and wet and dry flue gas desulfurization (FGD) [10, 12]. In addition, while rainfall parameters (e.g., wind, temperature, inversions, rainfall's duration, frequency, and intensity) and precipitation near the stacks affect the deposition of wet mercury (Hg), various meteorological factors such as wind speed affect the deposition of dry Hg [12, 13]. According to [9] and [14], even though most power plants were unlikely to cause any significant non-cancer risks to human health, arsenic (As), chromium (Cr), and lead (Pb) were the primary contributors to these risks. For cancer risks, the results showed that the pollutants would not cause any carcinogenic health effects to the population [9, 14]. The studies on air dispersion and risks from coal-fired power plants are summarized in **Table 1**.

Study	Country	Air dispersion and risk methods	Technology/power plant	Results
	Taiwan	ISCST	- 550 MW coal -fired power plant with ESP, FGD, and SCR - 10 stacks	- The average gaseous Hg (Hg^0 and Hg^{2+}) was 2.59–4.12 ng/m³ - The average particulate Hg (Hg^p) was 105–182 pg/m³ - The majority of the Hg from the stacks was in gaseous form, so the particulate form was very low - The maximum concentration of total Hg was from downwind site D (10 km from the plant) - The lowest concentration of total Hg was from upwind site A (11 km from the plant)
Lee and Keener Table [12]	USA	AERMOD and ISCST3	- 2 coal-fired power plants - 4 stacks for each plant	- The average annual atmospheric mercury concentration was 0.014–0.085 ng/m³ depending on each power plant and air dispersion modeling - The average annual dry Hg deposition was 3.62–6.25 μg/m² depending on each power plant and air dispersion modeling - The average annual dry Hg deposition was 0.35–13.73 μg/m² depending on each power plant and air dispersion modeling - Wet Hg deposition is influenced by rainfall parameters and precipitation near the stacks - Dry Hg deposition depends on meteorological factors - There were similar trends of Hg deposition between these two power plants
Mokhtar et al.	Malaysia	AERMOD and quality health	- 700 MW coal -fired power plant	- The predicted atmospheric As, Cd, Cr, and

Study	Country	Air dispersion and risk methods	Technology/power plant	Results
Table [14]		risk assessment (QHRA)	with ESP and FGD - 3 power plants	Pb concentrations were 1.84 × 10⁻⁴, 2.3 × 10⁻⁵, 5.38 × 10⁻⁴, 1.73 × 10⁻⁴ µg/m³
				- Hazard quotient (HQ) values of all pollutants concentration were less than one. This showed that the pollutants concentration were unlikely to cause any non-cancer risks to human health
				- For cancer risks, the results showed that the pollutants would not cause any carcinogenic health effects to the population which are at 1 km away from the power plants
French et al. Table [9]	U.S.	Screening assessment	426 coal-fired and 137 oil-fired power plants	- Cancer risks: 424 of the 426 coal-fired plants did not pose any risks. As and Cr were the primary contributors to these risks
				- Non-cancer risks: None of the emissions posed these risks
				- Hg emitted during coal-fired power generation is a potential concern since it is a persistent emission which contributes to the Hg levels especially in freshwater fish. Moreover, the emission mostly does not become deposited near the source but further away

Table 1. Summary of air dispersion studies on coal-fired power plants.

2.2. Health effects of typical power plant pollutants

Emissions from a typical coal-fired electricity-generating station without carbon capture technology include secondary aerosols such as heavy metals, nitrogen oxides (NOx), sulfur dioxide (SO₂), and non-methane volatile organic compounds (NMVOC), which pose risk to human health [15]. The emissions constitute air pollution and can be hazardous to human health [3]. Health effects of selected power plant pollutants are summarized and shown in **Table 2**.

Substances	Human toxicity		Limit value		Typical exposure within the plume	Comments
	Acute (short-term effects)	Chronic (long-term effects)	TWA (the 8-hour time-weighted average (TWA) limit	STEL (short term)/C ceiling	Emission factors (kg/mg coal)	
Sulfur dioxide (SO_2)	Lung irritant, triggers asthma, low birthweight in infants	Reduces lung function, associated with premature death	5000 ppm	15,000 ppm	2300	Contributes to acid rain and poor visibility
Nitrogen oxides (NOx)	Changes lung function, increases respiratory illness in children	Increases sensitivity to respiratory illnesses and causes permanent damage of lung	2 ppm	5 ppm	0.054	Forms ozone smog and acid rain. Ozone is associated with asthma, reduced lung function, adverse birth outcomes, and allergen sensitization
Nitrogen dioxide (NO_2)	Affect health exposure mortality	Decreased lung function in children, perhaps adults	N/A	N/A	4.25	–
Carbon monoxide (CO)	Increase frequency and severity of angina, headaches, exacerbation of cardio pulmonary dysfunction	Decrease work capacity in healthy adults, decrease alertness, flulike symptom in healthy adults, asphyxiation	N/A	1 ppm	N/A	–
Particulate matter (PM)	Asthma attacks, heart rate variability, heart attacks	Cardiovascular disease, lung inflam mation, premature death, decreased lung function	25 ppm	100 ppm	N/A	Fine-particle pollution from power plants is estimated to cut short the lives of 30,000 Americans each year
Hydrogen chloride (HCl)	Inhalation causes coughing, hoarse ness, chest pain, and inflammation of respiratory tract	Chronic occupational exposure is associated with gastritis, chronic lung inflammation, skin inflammation	N/A	N/A	0.308	–

Substances	Human toxicity		Limit value		Typical exposure within the plume	Comments
Hydrogen fluoride (HF)	Inhalation causes severe respiratory damage, severe irritation, and pulmonary edema	–	N/A	2 ppm	0.6	Very high exposures through drinking water or air can cause skeletal fluorosis
Arsenic (As)	Ingestion and inhalation affect the gastrointestinal system and central nervous system	Known human carcinogen with high potency. Inhalation causes lung cancer; ingestion causes lung, skin, bladder, and liver cancer. The kidney is affected following chronic inhalation and oral exposure	N/A	2 ppm	0.075	–
Cadmium (Cd)	Bronchial and pulmonary irritation, long-lasting impairment of lung function	Human carcinogen of medium potency, kidney injury, chronic inhalation, and oral exposure	$0.01\ mg/m^3$	N/A	0.000205	Other effects noted from chronic inhalation exposure are bronchiolitis and emphysema
Lead (Pb)	Abdominal (stomach) pain, seizures	Kidney injury, decrements in renal function, anemia, paralysis, nervous system issues, and loss of cognitive ability	$0.01\ mg/m^3$	N/A	0.0000255	–
Antimony (Sb)	Gastrointestinal symptoms (vomiting, diarrhea, abdominal pain, and ulcers)	Hemolysis with abdominal and back pain	$0.05\ mg/m^3$	N/A	0.00021	Acute inhalation is related to irritation of the respiratory tract and impaired pulmonary function
Barium (Ba)	Vomiting, perioral paresthesias, diarrhea, paralysis, hypertension, and cardiac dysrhythmias	Baritosis (coughing, wheezing, nasal irritation), kidney damage	$0.5\ mg/m^3$	N/A	0.000009	The health effects depend on the dose, water solubility, and route of exposure

Substances	Human toxicity		Limit value		Typical exposure within the plume	Comments
Chromium (Cr)	High exposure to chromium VI may result in damage to the kidneys, gastrointestinal bleeding, and internal bleeding	Known human carcinogen of high potency	0.5 mg/m^3	N/A	N/A	Chronic effects from industrial exposures are inflammation of the respiratory tract, effects on the kidneys, liver, and gastrointestinal tract
Beryllium (Be)	Erythema and edema of the lung mucosa. This will produce pneumonitis	Chronic beryllium disease or berylliosis	0.5 mg/m^3	N/A	0.0000395	The effects of beryllium vary depending on the concentration of the substance in the air and the duration of the air exposure
Copper (Cu)	Nausea, vomiting, abdominal pain, anemia	Symptoms of liver toxicity such as Wilson's disease, jaundice, and swelling	0.002 mg/m^3	0.01 mg/m^3	0.0000105	–
Cobalt (Co)	Allergic contact dermatitis	Asthma, carcinogenicity	1 mg/m^3	N/A	N/A	Two routes that cobalt can be absorbed: (1) oral and (2) pulmonary routes
Molybdenum (Mo)	–	A gout-like illness, higher serum uric acid levels, carcinogenicity	0.02 mg/m^3	N/A	0.00005	–
Manganese (Mn)	–	Parkinson's disease, clumsiness, tremors, speech disturbances, psychological disturbances, cough, bronchitis, lung disease	0.5 mg/m^3	N/A	N/A	No reports of human effects following acute effects to manganese are available
Selenium (Se)	Producing coughing, nosebleeds, dyspnea, bronchial spasms, bronchitis, and chemical pneumonia	Alkali disease (hair loss, erosion of the joints of the bones, anemia, etc.), cardiovascular disease	0.2 mg/m^3	N/A	0.000245	–

Substances	Human toxicity		Limit value		Typical exposure within the plume	Comments
	(lung irritation caused by toxins, gases, etc.)					
Nickel (Ni)	Skin rash, eczema	Asthma attacks, chronic bronchitis, reduced lung function, lung, and nasal sinus cancer (>10 mg nickel/m^3)	0.1 mg/m^3	N/A	0.00065	People can be exposed to nickel by breathing air and drinking water
Vanadium (V)	Cough, sputum, difficulty in breathing, ear, nose, and throat irritation, headache, palpitation	Cardiovascular disease	0.05 mg/m^3	N/A	0.00014	–
Mercury (Hg)	Inhalation exposure to elemental mercury results in central nervous system effects and effects on gastrointestinal tract and respiratory system	Methyl mercury ingestion causes developmental effects. Infants born to women who ingested methylmercury may perform poorly on neurobehavorial tests	0.2 mg/m^3	N/A	N/A	The major effect from chronic exposure to inorganic mercury is kidney damage
Volatile organic compounds (VOCs)	Irritation, neurotoxic effects, hepatotoxic effects, headache, nausea, irritation of eyes, respiratory system, drowsiness, fatigue	Asthmatic symptom, cancer	0.025 mg/m^3	N/A	0.0000415	–

Table 2. Health effects of typical coal-fired power plant pollutants (modified from Refs. Table [16–21]).

3. Methods of life cycle assessment (LCA)

LCA is a methodology that studies the whole life cycle of a product, often called the cradle-to-grave approach, in which complex systems are broken down into elementary flows. The life cycle assessment consists of four main stages: goal and scope definition, LCI analysis, life cycle impact assessment (LCIA), and interpretation. The phase of defining the goal and scope of an LCA study is important for it is at this stage that the requirements are set. The requirements determine the methodology, which can directly affect the results. The second phase of the LCA

involves construction of a flow model and an inventory analysis so as to provide inventory data for supporting the goal and scope defining in the study. The LCI model is generally shown as a flowchart; and LCI modeling consists of the construction of the flowchart, data collection, and the calculation procedure [22]. The third phase of LCIA aims to specify the environmental consequences in the inventory analysis process. This phase is normally applied to translate the environmental load, inputs, and outputs, based on the inventory results, into environmental impacts such as acidification, global warming potential, and ozone depletion. The last stage of an LCA is the interpretation of outcomes. At this stage, the main objectives include reaching conclusions and preparing recommendations for action. The conclusion should also be consistent with the goal and scope of the study.

The study focuses on using the emission outputs from the LCI step for calculating the emission concentration using air dispersion modeling. Then, the results are used to generate the cancer and non-cancer risks. All unit processes in each scenario of the carbon capture technology are modeled using engineering equations incorporated in a Microsoft® Excel spreadsheet.

4. Methods of air dispersion modeling and risk assessment of post- and oxy-fuel combustion CO_2 capture technologies

4.1. The selected technological boundaries

To assess health-related risks due to heavy metals, three scenarios are compared, which include (i) the conventional lignite-fired electricity generation station without CO_2 capture, (ii) the amine post-combustion CO_2 capture system, and (iii) the oxy-fuel combustion CO_2 capture

Figure 1. Boundary Dam Power Station (BDPS) in Estevan, Saskatchewan, Canada.

system. The lignite-fired electricity generation station at the BDPS in Estevan, Saskatchewan, Canada, was used in this study; the BDPS is shown in **Figure 1** [23, 24].

The three technologies are compared. These technologies include the following: (i) the conventional lignite-fired electricity generation station without CO_2 capture, (ii) the lignite coal-fired electricity-generating unit with an amine-based post-combustion capture system, and (iii) the oxy-fuel combustion CO_2 capture system. Each technology is described as follows. The conventional lignite-fired electricity generation station consists of (i) unit 3 at the BDPS, which generates 150 MW and is a tangentially fired subcritical boiler, and (ii) a dry ESP unit. The lignite coal-fired electricity-generating unit with an amine post-combustion capture system consists of the following: (i) unit 3 at the BDPS, which generates 150 MW and is a tangentially fired subcritical boiler, (ii) a dry ESP unit, (iii) a wet FGD unit, and (iv) a CO_2 capture and compression unit. The oxy-fuel combustion CO_2 capture system consists of the following: (i) an air separation unit (ASU) for cryogenic distillation, which is often commercially used for air separation, (ii) unit 3 at the BDPS, which generates 150 MW and is a tangentially fired subcritical boiler, (iii) a dry ESP unit, (iv) a wet FGD unit, and (v) a CO_2 purification and compression unit.

The oxy-fuel combustion CO_2 capture technology model is described in [6]. The post-combustion CO_2 capture technology model is presented in [8].

4.2. System boundary

The studied system is located at the BDPS unit 3 in Estevan, Saskatchewan, Canada. From this location, the emissions of heavy metals are predicted to occur in a circular pattern of 10 degrees increments with 25 points of 100 m on each increment. Each direction has 25 distances starting from 100 m and increases every 100 m. The location of the stack at the BDPS unit 3 is set as an origin of the emissions and designated as (0.0, 0.0).

4.3. Modeling air dispersion and risk

Since the objective of this study is to evaluate the risk to humans posed by the conventional coal-fired power plant, the post-combustion, and oxygen-based combustion systems specific to Saskatchewan, Canada, the evaluation was conducted using methodologies for assessing air pollution dispersion, cancer, and non-cancer risks. Two options were considered for implementing the air pollution dispersion methodology: AERMOD and CALPUFF. AERMOD is a steady-state Gaussian plume dispersion model, which is designed to predict near-field (<50 km) impacts [25]. The model aims to estimate and calculate how the pollutions, which are emitted from a source, can disperse in the atmosphere and travel across a receptor grid [26]. By contrast, CALPUFF is a non-steady-state meteorological and air quality modeling system, which can be applied to measure air quality from tens to hundreds of kilometers [27, 28]. The model consists of preprocessing and post-processing programs that can be categorized into three main components: (1) a meteorological model, (2) an air dispersion model, and (3) post-processing packages for the meteorological, concentration, and deposition data output [29]. Both AERMOD and CALPUFF were developed by the US EPA. Since the Government of

Saskatchewan provides the meteorological data specific to Estevan required in the AERMOD model, and AERMOD has been widely used for predicting near-field impacts of chemical pollutants, the AERMOD model is suitable because this study aims to evaluate the risks to health that people who live near the power station face.

Due to the limited available data on the heavy metals, the equations for calculating cancer and non-cancer risks from [30, 31] were chosen as the most appropriate tools for conducting the risk analysis.

4.3.1. Modeling air dispersion

As previously stated, AERMOD is a steady-state Gaussian plume dispersion model, which is designed to predict near-field (or less than 50 km)impacts in both simple and complex terrains as shown in **Figure 2** [25, 32]. The model recognizes the manner in which the pollutants emitted from a source are dispersed in the atmosphere and travel across a receptor grid [26].
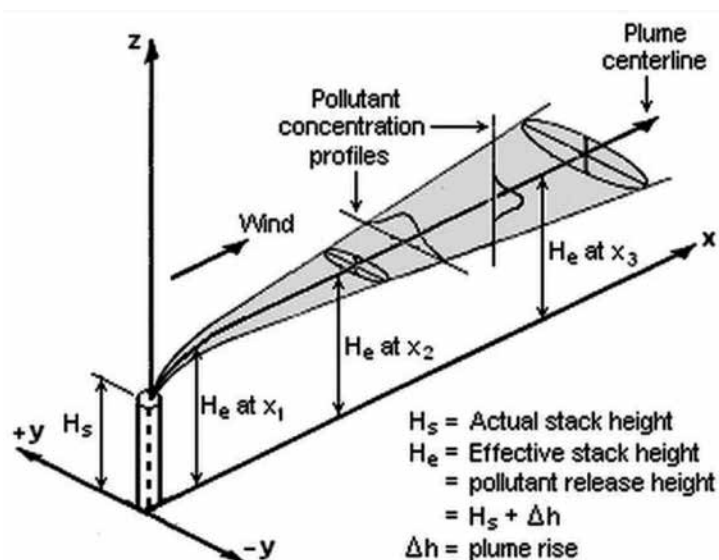
Figure 2. Steady-state Gaussian plume dispersion model in AERMOD [32].

The main data requirements for AERMOD include AERMET, or meteorological data in Estevan, emission rates released from the selected stack, stack height, exit temperature and velocity of the selected emission, and inside stack diameter. The sources of data consist of (i) the meteorological dataset specific to Estevan required in the AERMOD model, which has been provided by the Government of Saskatchewan (www.environment.gov.sk.ca); (ii) the stack data for the "no capture" and "post-combustion" scenario provided by the Saskatche-wan Power Corporation (SaskPower) and the dataset of the oxy-fuel combustion generated using the IECM software version 8.0.2 (Trademark of Carnegie Mellon University, USA), and

(iii) the emission rates from the power plant obtained from the LCA studies of a conventional coal-fired power plant, a post-combustion, and an oxy-fuel combustion CO_2 capture processes [6–8]. The meteorological data from years 2003–2007 were used for the AERMOD modeling due to the limitations in available data. The stack data and emission rates are summarized in **Table 3**.

Coal-fired power plant	BDPS unit 3 (without CO_2 capture)	BDPS unit 3 (with oxy-fuel combustion CO_2 capture)	BDPS unit 3 (with post-combustion CO_2 capture)
Stack height (m)	91.44	91.44	91.44
Stack diameter (m)	4.27	4.27	4.27
Exit gas velocity (m/sec)	18.1	15.09	18.1
Exhaust gas temperature (K)	436.15	310.93	436.15
Mercury (Hg)	0.001902781	–	0.001675417
Antimony (Sb)	0.000170833	1.70833E−06	3.41667E−06
Arsenic (As)	0.002041667	0.000018375	0.00003675
Barium (Ba)	0.000541667	5.41667E−06	1.08333E−05
Beryllium (Be)	6.66667E−05	3.33333E−07	6.66667E−07
Cadmium (Cd)	0.000170833	3.41667E−06	6.83333E−06
Chromium (Cr)	0.002458333	0.0000295	0.000059
Cobalt (Co)	0.0002875	0.000002875	0.00000575
Copper (Cu)	0.000958333	2.97083E−05	5.94167E−05
Lead (Pb)	0.00125	0.0000125	0.000025
Manganese (Mn)	0.000179167	1.25417E−06	2.50833E−06
Molybdenum (Mo)	0.001583333	1.58333E−05	3.16667E−05
Nickel (Ni)	0.002416667	3.38333E−05	6.76667E−05
Selenium (Se)	0.017083333	0.0007175	0.001435
Vanadium (V)	0.003666667	2.93333E−05	5.86667E−05

Table 3. Stack features and emission rates.

A comparison of the three scenarios revealed that the higher temperatures, which cause more atmospheric lift, occur with the stacks in the "no capture" and the "post-combustion capture" scenarios. However, the flow velocity in the "post-combustion capture" scenario should have been slightly lowered because of the pressure drop in the unit processes. This study used the same flow velocity both in the "no capture" and the "post-combustion capture" scenarios because this study has adopted the data on the exhaust gas velocity and temperature from SaskPower, which was the only source of data available. The "oxy-fuel combustion" scenario showed lower exhaust gas velocity and temperatures due to the recycling of the flue gas and

the CO_2 compression and purification unit. The data on exit gas velocity was obtained from the SaskPower Web site for the "no capture" and "post-combustion" scenarios, while the oxy-fuel combustion data were results taken from IECM modeling.

4.3.2. Analysis of cancer and non-cancer risks analysis

The risk calculation involves an estimation of the cancer and non-cancer risks related to heavy metals, which can become inhaled contaminants. The emission data for the "no capture" and the two "capture" scenarios are taken from the LCI results in [6–8]. Based on the data, the emission concentrations on the ground were generated using AERMOD, and then, the data were used for evaluating the cancer and non-cancer risks. The equations recommended for estimating cancer and non-cancer risks are taken from [30, 31].

4.3.2.1. Long-term cancer risk

While cancer risks can be associated with both inhalation and ingestion, this study only took the risk related to inhalation into consideration. The unacceptable cancer risk is the risk higher than 1,000,000 [9, 33]. In other words, a cancer risk which is higher than 0.000001 will cause carcinogenic effects, which is an undesirable outcome. The unit risk factor (URF) data were taken from the toxicity values for inhalation exposure shown on the New Jersey Department of Environmental Protection Web site (www.nj.gov). The cancer risk via the inhalation pathway can be calculated with the following equation:

$$Cancer\ risk = EC*URF \tag{4.1}$$

where EC = Exposure air concentration ($\mu g/m^3$) and URF = Unit risk factor ($\mu g/m^3$)$^{-1}$.

4.3.2.2. Long- and short-terms non-cancer risk

The exposure to non-cancer risk due to direct inhalation can be estimated using the hazard quotient (HQ) approach, which involves a ratio for estimating chronic dose/exposure level to the reference concentration (RfC), an estimated daily concentration of emissions in the air [30, 34]. There are two main types of RfC values associated with long-term and short-term effects. The RfC data were taken from the toxicity values for inhalation exposure shown on the New Jersey Department of Environmental Protection Web site (www.nj.gov). HQ values equal to or less than one are referred to as having little or no adverse effect [34]. By contrast, a HQ value that exceeds one implies that the emissions have reached a level of concern [35]. However, since the HQ is not a probability of risk, it does not matter how large the HQ value is, only whether or not the HQ value exceeds one [34]. For example, a quotient of 0.01 does not mean that there is a one in a hundred chance that the effect will occur. The HQ value is calculated using the following equation.

$$HQ = EC\ /\ RfC \tag{4.2}$$

where HQ = Hazard quotient (unitless), EC = Exposure air concentration ($\mu g/m^3$), and RfC = Reference concentration ($\mu g/m^3$).

5. Results

5.1. Results from AERMOD

The study examined the air dispersion modeling of the "no capture" and the two "capture" scenarios. For cancer and non-cancer risks, the maximum 24-hour and 1-hour average concentration values of heavy metals were used for long-term and short-term exposures, respectively. The maximum 24-hour concentration values generated from AERMOD of the "no capture," "post-combustion CO_2 capture," and "oxy-fuel combustion CO_2 capture" scenarios are shown in **Table 4**. For short-term effects, the maximum 1-hour concentration values generated from AERMOD of the "no capture," "post-combustion CO_2 capture," and "oxy-fuel combustion CO_2 capture" scenarios are shown in **Table 5**. It can be seen from the two tables that the maximum 24-hour and 1-hour average concentrations of the heavy metals of the "no capture" scenario, respectively, show the highest concentrations compared to the other two scenarios. This shows that when the CO_2 capture technologies are applied, lower concentrations of Hg and heavy metals will be emitted into the air. These emissions are captured by the pollution control units provided in the CO_2 capture technologies, and distribution in the atmosphere is controlled by parameters such as the stack height, exhaust gas temperature, and exit gas velocity, as shown in **Table 3**.

Substances	Concentrations		
	No capture	Oxy-fuel combustion	Post-combustion
Hg	4.72E–02	0	4.15E–02
As	5.06E–02	1.08E–03	9.1E–04
Ba	1.34E–02	3.2E–04	2.7E–04
Be	1.65E–03	2.0E–05	2.0E–05
Cd	4.24E–03	2.0E–04	1.7E–04
Cr	6.1E–02	1.73E–03	1.46E–03
Co	7.14E–03	1.7E–04	1.4E–04
Cu	2.37E–02	1.74E–03	1.47E–03
Pb	3.10E–02	7.3E–04	6.2E–04
Ni	5.99E–02	1.99E–03	1.68E–03
Se	4.23E–01	4.21E–02	3.56E–02
V	9.1E–02	1.72E–03	1.46E–03

Table 4. The maximum 24-hour average concentrations of the heavy metals of the "no capture" and the two "capture" scenarios in 2003–2007 ($\mu g/m^3$).

Substances	Concentrations		
	No capture	Oxy-fuel combustion	Post-combustion
Hg	4.16E–01	0	3.66E–01
As	4.47E–01	8.43E–03	8.05E–03
Ba	1.18E–01	2.48E–03	2.37E–03
Be	1.46E–02	1.5E–04	1.5E–04
Cd	3.74E–02	1.57E–03	1.5E–03
Cr	5.38E–01	1.35E–02	1.29E–02
Co	6.29E–02	1.32–03	1.26E–03
Cu	2.09E–01	1.36E–02	1.3E–02
Pb	2.73E–01	5.73E–03	5.47E–03
Ni	5.29E–01	1.55E–02	1.48E–02
Se	3.74	3.29E–01	3.14E–01
V	8.02E–01	1.34E–02	1.28E–02

Table 5. The maximum 1-hour average concentrations of the heavy metals of the "no capture" and the two "capture" scenarios in 2003–2007 ($\mu g/m^3$).

The oxy-fuel combustion system gives out less emission at a lower flow velocity, so the emissions fall on the ground closer to the stack and there are less emissions further away. By contrast, the post-combustion system gives out higher emissions at a higher velocity, which enables the emissions to travel further away; the higher temperature of the flue gas also causes atmospheric lift of the emissions. As a result, the emissions are more evenly distributed over a wider area further away from the stack, and their concentrations are lower.

5.2. Results from cancer and non-cancer risks related to heavy metals

The missing inhalation URF and RfC values limit the calculations of cancer and non-cancer risks for some metals. Cancer and non-cancer risk results are shown in **Table 6** and **Table 7**, respectively. **Tables 6** indicates that the emissions from the stack in each of the three scenarios pose cancer risks of less than one chance in a million (1×10^{-6}). However, there are two emissions, which include As and Cr, from the "no capture" scenario that pose cancer risks due to inhalation with a chance greater than 1×10^{-6}. In terms of non-cancer risks, the inhalation exposures are estimated by the HQ value, a ratio to estimate chronic dose/exposure level to RfC, an estimated daily concentration of emissions in air. The results shown in **Table 7** display that all HQ values are less than one. When the HQ values are less than one, this indicates that pollutant concentrations from the three stacks are unlikely to correlate with any non-cancer-related health concerns.

Substances	Inhalation unit risk factor (URF) $(\mu g/m^3)^{-1}$	Cancer risk		
		No capture	Oxy-fuel combustion	Post-combustion
Hg	–	–	–	–
As	4.3E–03	1.45E–06	3.09E–08	2.61E–08
Ba	–	–	–	–
Be	2.4-E03	2.64E–08	3.20E–10	3.20E–10
Cd	4.2E–03	1.18E–07	5.6E–09	4.76E–09
Cr	1.2E–02	4.88E–06	1.38E–07	1.16E–07
Co	9E–03	4.28E–07	1.02E–08	8.4E–09
Cu	–	–	–	–
Pb	1.2E–05	2.48E–09	5.84E–11	4.96E–11
Ni	–	–	–	–
Se	–	–	–	–
V	–	–	–	–

Table 6. Cancer risks of heavy metals.

Substances	Long term				Short term			
	RfC $(\mu g/m^3)$	Non-cancer risk			RfC $(\mu g/m^3)$	Non-cancer risk		
		No capture	Oxy-fuel combustion	Post-combustion		No capture	Oxy-fuel combustion	Post-combustion
Hg	0.3	1.05E–03	0	9.24E–04	–	–	–	–
As	0.015	2.25E–02	4.8E–04	4.04E–04	0.2	1.49E–02	2.81E–04	2.68E–04
Ba	–	–	–	–	0.5	1.58E–03	3.31E–05	3.16E–05
Be	0.4	5.5E–04	6.67E–06	6.67E–06	–	–	–	–
Cd	0.02	1.41E–03	6.67E–05	5.56E–05	–	–	–	–
Cr	–	–	–	–	–	–	–	–
Co	0.006	7.93E–03	1.88E–04	1.55E–04	–	–	–	–
Cu	–	–	–	–	100	1.39E–05	9.09E–07	8.67E–07
Pb	–	–	–	–	0.1	1.82E–02	3.82E–04	3.65E–04
Ni	0.05	7.99E–03	2.65E–04	2.24E–04	6	5.87E–04	1.72E–05	1.65E–05
Se	20	1.41E–04	1.40E–05	1.18E–05	–	–	–	–
V	0.1	6.06E–03	1.14E–04	9.73E–05	–	–	–	–

Table 7. Long- and short-term inhalation exposures of heavy metals.

6. Discussion

The carbon capture technology is one of the most widely discussed solutions for cutting GHG emissions which are mostly generated from electrical generation that uses fossil fuels (e.g., oil, coal, and natural gas, which are regarded as the world's primary source of energy). According to [36], fossil fuels will be continuously used to supply energy globally for at least the next few decades, especially with the recent development of shale gas in many regions of the world. In this scenario, without a proper control technique, the CO_2 atmospheric emissions will continue to increase and pose an even more serious threat to people and the environment. To cope with this problem, the adoption and use of an effective CO_2 capture technology have become an important approach in ensuring the reduction CO_2 emissions. Consequently, it is important to conduct risk assessment to ensure safety of the carbon capture technology. Understanding those risks can support the formulation of standards and regulatory frameworks required for large-scale application of the carbon capture technology [5]. Greater emissions of carbon dioxide poses hazards to human health because inhaling concentrations of CO_2 emissions around 3–5% will pose risks to human health [37]. Inhaling concentration higher than 15% can be fatal. The health, safety, and environmental (HSE) risk of the fossil-fuel-based electrical generation system can be determined to a large extent by both the total amount of CO_2 lost and the maximum rate of CO_2 lost in the system [2]. The health-related damage associated with emissions from coal-fired electricity-generating plants can vary, depending on a number of factors including the facilities, the function of the plant, the site, and population characteristics [38].

Different studies focus on different kinds of risks associated with the process of carbon capture such as (1) cancer and non-cancer risks; (2) population exposure per unit of emissions, which is associated with atmospheric condition, the population size, and their proximities to the emissions; (3) social and mental impacts; and (4) accidents and deaths [9, 14, 15, 39–42]. According to [9], among the emissions from coal-fired electricity-generating plants, As and Cr were the main contributors to cancer risks, and HCl, Mn, HF, and Hg contributed to the non-cancer risks. The coal combustion process can also release many toxic elements, which include As, Hg, Cd, Pb, Se, and Zn, and among these, Hg is of the most concern [15]. According to [43], the population in Estevan has an exceptionally high rate of asthma. In [44], the study compares the human health risks associated with SO_2, NO_2, and $PM_{2.5}$ of the oxy-fuel carbon dioxide capture with those from the post-combustion CO_2 capture technology, and the study reveals that the oxy-fuel system posed fewer human health risks because this technology captures more emissions. In [44], the study fills the gap in research because none of the past studies emphasize the human health impacts due to heavy metals associated with the BDPS in Estevan, Saskatchewan, Canada. This study produces useful data on human health risk and help decision makers quantify the impact of different CO_2 capture technologies. From a practical perspective, the study provides support for efforts aimed at improving the air quality in the Estevan region.

7. Conclusion

Since the coal-fired electricity generation plant is widely regarded as a significant source of air pollution, the adoption of the carbon capture technology is a potential solution for reducing emissions. However, the carbon capture technology requires additional energy for its operation which results in lowering the overall efficiency of the electricity-generating plant. More fossil fuel per unit of electricity generated is needed to compensate for the lost capacity, but the higher requirement also necessitates a higher level of emissions and resource consumption. Since safety of the carbon capture technology is an important public concern, a risk analysis of the carbon capture technology was conducted. While risk is normally defined as the potential of an unwanted negative consequence or event [17], risk analysis is a tool used to form, structure, and collect information to identify existing hazardous situations and report potential problems or the type and level of the environmental health and safety risk [36].

This study focuses on examining the health impacts of the conventional coal-fired generation station without CO_2 capture, with post-combustion and oxy-fuel combustion CO_2 capture technologies. The study analyzed the cancer and non-cancer risks to human health based on the data of air pollutants from heavy metals obtained from the LCA models [6–8]. The risks associated with these pollutants are calculated for the three CO_2 capture scenarios of (i) "no capture," (ii) "post-combustion CO_2 capture," and (iii) "oxy-fuel combustion CO_2 capture."

7.1. Summary of air dispersion modeling

The maximum 24-hour and 1-hour average concentration values of Hg and heavy metals are used for assessing the long-term and short-term exposures, respectively. The results show that, in the "no capture" scenario, the maximum 24-hour and 1-hour average concentrations of the Hg and heavy metals, respectively, show the highest concentrations compared to the two "capture" scenarios. This shows that these emissions are captured by the pollution control units of the CO_2 capture technologies and the less concentrated Hg and heavy metals consequently will be emitted into the air. The air dispersion modeling, which generates emission concentrations, depends not only on the amount of emissions but also on other parameters such as the stack height, exhaust gas temperature, and exit gas velocity. Compared to the post-combustion system, the oxy-fuel combustion system gives out less emission at a lower flow velocity, so the emissions fall on the ground closer to the stack. As a result, there are less emissions further away.

7.2. Summary of risk analysis

The analysis results shown in **Table 6** indicate that the emissions from the three stacks generally posed cancer risks of less than one chance in a million (1×10^{-6}). However, there are emissions from two elements in the "no capture" scenario that pose cancer risks of more than 1×10^{-6}; As and Cr are the primary contributors to these risks. In terms of non-cancer risks, the results show that all HQ values are less than one. This indicates that the pollutant concentration from the three stacks will not cause any non-cancer health issues.

A limitation in the cancer and non-cancer risks calculation is that data on URF and RfC associated with some types of heavy metals are not available. In future studies, this limitation can be addressed. Generally, it can be concluded that for electricity generation with carbon capture, even though there are increases in adverse health impacts associated with soil and water pollution, the broad distribution of health impacts associated with atmospheric pollutants is significantly reduced. We believe the benefits to human health outweigh the negative of increased emissions.

Acknowledgements

Author details

Jarotwan Koiwanit[1], Anastassia Manuilova[2], Christine Chan[1*], Malcolm Wilson[2] and Paitoon Tontiwachwuthikul[1]

*Address all correspondence to: chanchristine888@gmail.com

1 Faculty of Engineering and Applied Science, University of Regina, Saskatchewan, Canada

2 ArticCan Energy Services, Regina, Saskatchewan, Canada

References

[1] IPCC. Summary for policymakers in climate change 2014: Impacts, adaptation, and vulnerability. New York, USA: Intergovernmental Panel on Climate Change; 2014.

[2] Gerstenberger M, Nicol A, Stenhouse M, Berryman K, Stirling M, Webb T, Smith W. Modularised logic tree risk assessment method for carbon capture and storage projects. Energy Procedia. 2009; 1(1): 2495–2502.

[3] Trabucchi C, Donlan M, Wade S. A multi-disciplinary framework to monetize financial consequences arising from CCS projects and motivate effective financial responsibility. International Journal of Greenhouse Gas Control. 2010; 4(2): 388–395.

[4]   Statistics Canada. Census agglomeration of Estevan, Saskatchewan. 2015 [Internet]. Available from: https://www12.statcan.gc.ca/census-recensement/2011/as-sa/fogs-spg/Facts-cma-eng.cfm?LANG=Eng&GK=CMA&GC=750. Accessed on 30 August 2015.

[5]   Damen K, Faaij A, Turkenburg W. Health, safety and environmental risks of underground CO_2 sequestration. (No. NWS-E-2003-30). Netherlands: Copernicus Institute for Sustainable Development and Innovation; 2003.

[6]   Koiwanit J, Manuilova A, Chan C, Wilson M, Tontiwachwuthikul P. A life cycle assessment study of a hypothetical Canadian oxy-fuel combustion carbon dioxide capture process. International Journal of Greenhouse Gas Control. 2014; 28: 257–274.

[7]   Koiwanit J, Piewkhaow L, Zhou Q, Manuilova A, Chan C W, Wilson M, Tontiwachwuthikul P. A life cycle assessment study of a Canadian post-combustion carbon dioxide capture process system. The International Journal of Life Cycle Assessment. 2014; 19(2): 357–369.

[8]   Manuilova A. Evaluation of environmental performance of carbon capture and storage project in Canada using life cycle assessment methodology [thesis]. Regina: University of Regina; 2011.

[9]   French C, Peters W, Maxwell B, Rice G, Colli A, Bullock R, Cole J, Heath E, Turner J, Hetes B, Brown D C, Goldin D, Behling H, Loomis D, Nelson C. Assessment of health risks due to hazardous air pollutant emissions from electric utilities. Drug and Chemical Toxicology. 1997; 20(4): 375–386.

[10] Wu Y, Rahmaningrum D, Lai Y, Tu L, Lee S, Wang L, Chang-chien G. (Mercury emissions from a coal-fired power plant and their impact on the nearby environment. Aerosol and Air Quality Research. 2012; 12: 643–650.

[11] Srivastava R K, Hutson N, Martin B, Princiotta F, Staudt J. Control of mercury emissions from coal-fired electric utility boilers. Environmental Science & Technology. 2006; 40(5): 1385–1393.

[12] Lee S, Keener T C. Dispersion modeling of mercury emissions from coal-fired power plants at Coshocton and Manchester, Ohio. Ohio Journal of Science. 2008; 108(4): 65–69.

[13] Tudose T, Moldovan F. Characteristics of heavy rainfall parameters in the north-western Romania. Aerul şi Apa: Componente ale Mediului. 2011; 91–98.

[14] Mokhtar M M, Hassim M H, Taiba M R, Lim S Z, Sahani M. Health risk assessment in coal-fired power plant in Malaysia. In: Proceedings of the 6th International Conference on Process Systems Engineering (PSE ASIA); 2013. p. 147–152.

[15] Castleden W M, Shearman D, Crisp G, Finch P. The mining and burning of coal: effects on health and the environment. The Medical Journal of Australia. 2011; 195(6): 333–335.

[16] CDC. Fourth national report on human exposure to environmental chemicals. Atlanta, GA, USA: Centers for Disease Control and Prevention; 2009.

[17] Elizabeth L A, Roy E A. Risk assessment and indoor air quality. New York, USA: Lewis Publishers; 1998.

[18] Hu H. (2002). Human health and heavy metals exposure. In: McCally M, editor. Life support: The environment and human health; MIT Press. Cambridge, Massachusetts. 2002. p. 65–82.

[19] Keating M. Cradle to grave: the environmental impacts from coal. Boston, MA, USA: Clean Air Task Force; 2001.

[20] NH DES. Copper: health information summary. Concord, NH, USA: New Hampshire Department of Environmental Services; 2013.

[21] US EPA. Selenium compounds. 2000. [Internet]. Available from:http://www.epa.gov/ttnatw01/hlthef/selenium.html. Accessed on 15 August 2013.

[22] Baumann H, Tillman A. The hitch hiker's guide to LCA. An orientation in life cycle assessment methodology and application. United States of America: Studentlitteratur; 2004.

[23] Beacon news group Canada. SaskPower launches world's largest carbon capture project. Edmonton Beacon; 2014.

[24] Environment Canada. Forecast regions - Saskatchewan. 2013. [Internet]. Available from: http://www.ec.gc.ca/meteo-weather/default.asp?lang=En&n=CE708E88-1. Accessed on 21 November 2014.

[25] US EPA. Summary of public comments: 10th conference on air quality modeling. (No. EPA - HQ - OAQ - 2012 - 0056). U.S.: US EPA, Washington, DC; 2012.

[26] Heckel P F, LeMasters G K. The use of AERMOD air pollution dispersion models to estimate residential ambient concentrations of elemental mercury. Water, Air, & Soil Pollution. 2011; 219(1–4): 377–388.

[27] Hoeksema G, Onder K, Unrau G. A comparison of Aermod and Calpuff models for regulatory dispersion modelling in the alberta oil sands region. Air and Waste Management Association Annual Meeting Conference and Exhibition. 2011; 3: 2035–2044.

[28] US EPA. CALPUFF modeling system. 2013. [Internet]. Available from: http://www.epa.gov/scram001/dispersion_prefrec.htm. Accessed on 4 April 2014.

[29] Scire J S, Strimaitis D G, Yamartino R J. A user's guide for the CALPUFF dispersion model. Concord, MA, USA: Earth Tech, Inc; 2000.

[30] US EPA. Chapter 7: Characterizing risk and hazard. Human health risk assessment protocol (pp. 7-1-7-15). 2005; US EPA, Washington, DC.

[31] US EPA. Risk assessment guidance for superfund. volume I: Human health evaluation manual: (Part F, supplemental guidance for inhalation risk assessment). (No. EPA-540-R-070-002). Washington, DC: US EPA; 2009.

[32] Beychok M. Air pollution dispersion modeling; 2012. Available from: http://www.eoearth.org/view/article/169860/ [Accessed 2014-11-21].

[33] ATSDR. Public health assessment guidance manual (2005 update): Appendix F: Derivation of comparison values [Internet]; 2005. Available from: http://www.atsdr.cdc.gov/hac/PHAManual/appf.html [Accessed: 2014-12-15].

[34] US EPA. Ecological risk assessment step 2 [Internet]; 2011. Available from: http://www.epa.gov/R5Super/ecology/erasteps/erastep2.html [Accessed: 2014-12-15].

[35] Kincaid L E, Davis G A, Meline J. Cleaner technologies substitutes assessment – A methodology and resource guide. Washington, DC: US EPA; 1997.

[36] Suebsiri J. A model of carbon capture and storage with demonstration of global warming potential and fossil fuel resource use efficiency [thesis]. Regina: University of Regina; 2010.

[37] Lilliestam J, Bielicki J M, Patt A G. Comparing carbon capture and storage (CCS) with concentrating solar power (CSP): Potentials, costs, risks, and barriers. Energy Policy. 2012; 47: 447–455.

[38] Levy J I, Baxter L K, Schwartz J. Uncertainty and variability in health-related damages from coal-fired power plants in the United States. Risk Analysis. 2009; 29(7): 1000–1014.

[39] Gjernes E, Helgesen L I, Maree Y. Health and environmental impact of amine based post combustion CO_2 capture. Energy Procedia. 2013; 37: 735–742.

[40] Nielsen C J, Herrmann H, Weller C. Atmospheric chemistry and environmental impact of the use of amines in carbon capture and storage (CCS). Chemical Society Reviews, 2012; 41(19): 6684–6704.

[41] Preiss P, Roos J, Friedrich R. Assessment of health impacts of coal fired power stations in Germany. Stuttgart, Germany: Institute for Energy Economics and the Rational Use of Energy (IER); 2013.

[42] Senior C L, Morris W, Lewandowski T A. Emissions and risks associated with oxyfuel combustion: state of the science and critical data gaps. Journal of the Air & Waste Management Association. 2013; 63(7): 832–843.

[43] The University of Saskatchewan Airways Research Group. The impact of airborne environmental contaminants on respiratory public health in Saskatchewan; 2012. Unpublished manuscript.

[44] Koiwanit J. Evaluation of environmental performance of hypothetical Canadian oxy-fuel combustion carbon capture with risk and cost analyses [thesis]. Regina: University of Regina; 2015.

About the Concept of the Environment Recycling— Energy (ERE) in the Romanian Steel Industry

Adrian Ioana and Augustin Semenescu

Abstract

This paper takes as its starting point an analysis of the ecological functioning of the electric arc furnace (EAF). Thus, we present a classification of emissions generated by EAF, including limits of variation in chemical composition of "dust" issued by EAF in various countries and limit values for permissible concentrations of these emissions.The paper presents and analyzes various abstraction and treatment-related emissions for hipo-polluting operation of EAF. In this chapter, the correlations between macro system represented by metallurgical environment and interacting systems: System-Energy-Recycling Environment (ERE), Ecological system (ECO), and Recycling, Reclamation System (REC-REV) are presented. These correlations are presented in the spirit of sustainable development concepts (DC) and total quality (TQ).

Keywords: environment-recycling-energy, metallurgical process technology, ecological system

1. Introduction

Reducing the amount of emissions and greenhouse gas immissions is an important environmental goal, including specific achievement to ensure the optimal concept of sustainable development.

The Electric Arc Furnace (EAF) for steel development is a powerful polluter. From this point of view, studying and optimizing the functioning of this complex metallurgical aggregate, including the conception of ERE, are of special importance. These activities of study and optimization ensure the optimal conditions for sustainable development.

Metallurgical process is a macroenvironment characterized mainly by the following systems:

- Metallurgical Process Technology system (MPT)—it is analyzed and defined by technological parameters and technological procedures applied.

- The Environment Energy Recycling System (EER)—it defines and characterizes the energy resources necessary for the transformations sources and the metallurgical processes.

- The Ecological System (ECO)—it refers to the organic processing systems pollutant outputs from MPT and EER.

- The Recycling and Revaluation System (REC-REV)—it refers to the energy and material transformations that occur within process flows. This system consists of two subsystems in turn, namely:

- The recycling subsystem (the capitalization) energy (R_E); this subsystem studies and makes more efficient the recycling of energy both within the same ecosystem and within the energetic exchanges between the ecosystems that are interdependent.

- The recycling subsystem (the capitalization) of materials (R_M); this subsystem is directly correlated with energy recycling subsystem, and it represents at the same time a qualitative and quantitative measure of it.

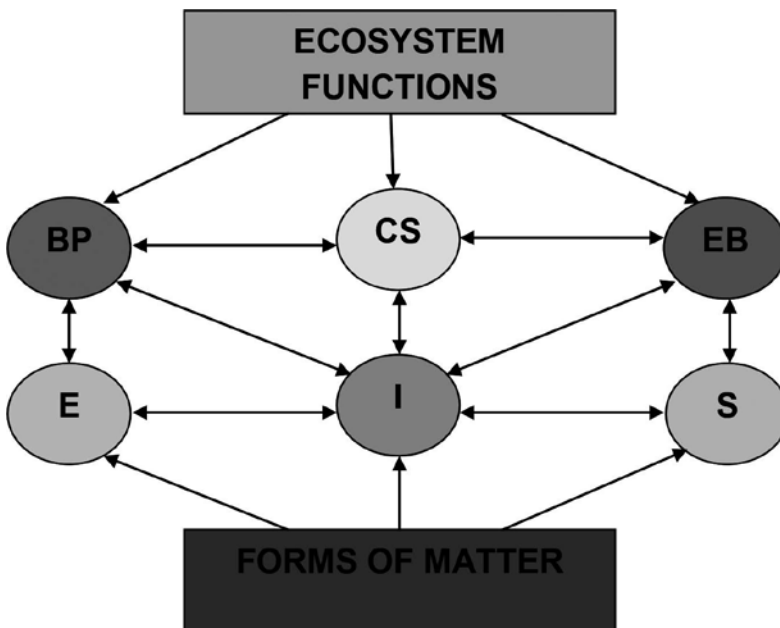An ecosystem performs three important functions. These functions are as follows:

Figure 1. The correlations between an ecosystem functions and forms of matter. Source: own research. BP—the biological productivity; CS—the circulation of substance; EB—the ecological balance; E—energy; I—information; and S—substance.

- The biological productivity (BP)—the biological productivity of an ecosystem is directly dependent both on the quality of the biotope (geographical environment) and on the biocenosis (all living organisms).

- The circulation of substance (CS)—this function of the ecosystem refers to the exchange of materials both within the same ecosystem and between different ecosystems that are interdependent.

- The ecological balance (EB)—is a function of quantification (quantitative determination) of the exchanges of matter and energy within an ecosystem.

The functions of an ecosystem must be analyzed in relation to the transformations through the three forms of matter:

- Energy (E)—energy as a form of matter is a measure of its quality.

- Information (I)—the information is the genetic carrier of the matter; it also characterizes the history and evolution of the respective matter.

- Substance (S)—it is a way of quantifying the matter. **Figure 1** shows the correlations between an ecosystem functions and forms of matter.

A brief explanation is useful to the ecosystem functions:

- The transformation of energy is illustrated by the size and variation in biological productivity.

- The circuit of macroelements reflects the changes of the substance.

- The ecological balance is an expression of the size of information.

2. The correlations of MPT-ERE-ECO-REC-REV

Based on the concepts of sustainable development (SD) and total quality (TQ), the effective analysis of a process and metallurgy must put on the forefront quantify correlations MPT-EER-ECO-REC-REV. In **Figure 2**, we present these correlations scheme.

The ecosystem, by definition, is a group consisting of biotopes, which sets a whole different relationships, both between organisms and between organisms and between abiotic factors.

This first definition of ecosystem requires a specific definition and an explanation of other concepts, such as:

- Biotope

- Biocenosis

- Abiotic

The Biotope is defined as the geographical environment in which there lives a group of living organisms (humans, plants, animals, etc.) in homogeneous conditions.
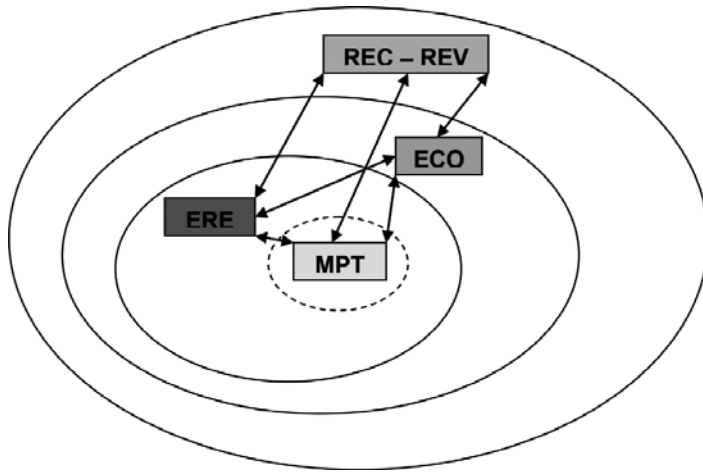
Figure 2. The correlations between the systems of MPT, EER, ECO and REC-REV to ensure concepts of DD and CT. Source: own research. MPT—The Metallurgical Process Technology; ERE—The Environment-Recycling Energy System; ECO—The Ecological system; REC–REV—The Recycling and Recovery of the System Recovery; SD—Sustainable Development; TQ—Total Quality.

The Biocenose represents all living organisms that inhabit a particular geographical environment (biotope).

The Abiotic refers to something lifeless, incompatible with life.

It is based on this first definition in **Figure 3**. This is the diagram of the ecosystem.
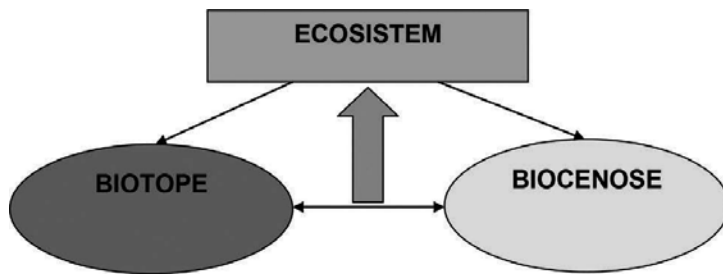

Figure 3. The diagram of the ecosystem. Source: [5].

The following general concepts on which they define in the automatization domeny is the System Ecometalurgic (SE).

The System Ecometallurgic is an ecosystem of custom-specific conditions and technologies in metallurgy (industry metallic materials—ferrous and nonferrous), characterized by a geographic environment and an specific industry (biotope) and by groups of living organisms (people, plants, and animals) that inhabit this environment (biocenosis).

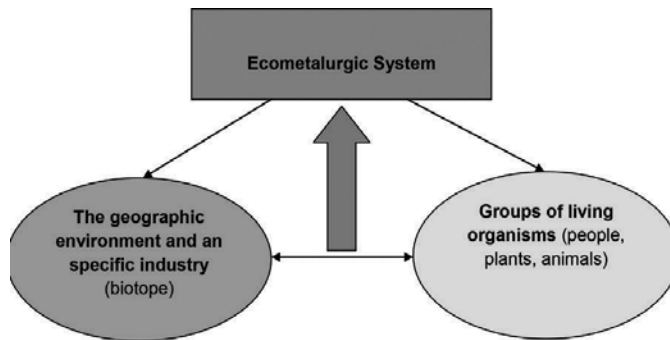**Figure 4** shows a schematic diagram of the ecometalurgic system.

Figure 4. Scheme of ecometallurgic system (ES). Source: own research.

3. The Classification and Characterization of the Ecometallurgic Systems (ES)

We define and characterize two types of ecometallurgic systems (ES), namely:

a. Monovariabile SE (SEMo)

b. Multivariabile SE (SEMu)

3.1. The characterization

a. Monovariable SE (SEMo)—it is characterized by a single magnitude input (u(t); m(t)), a single magnitude output (y(t)); and a single magnitude of perturbation (p(t)).

In **Figure 5**, we present a schematic diagram of an monovariabile ecometallurgic system (SEMO).

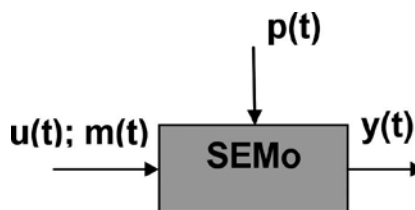**Figure 5.** The schematic diagram of an monovariable ecometallurgic system (SEMo). Source: [5]. u(t); m(t)—magnitude input; y(t)—magnitude output; and p(t)—magnitude of perturbation.

SE Monovariable—it is used to study mathematical modeling and simulation. Given the complexity of the metallurgy, simulation and mathematical modeling can have a great importance.

a.   SE Multivariable (SEMu)—it is characterized by several dataset input quantities ($\sum u, m_{i(t)}$), more outputs—the set of output quantities ($\sum y_{j(t)}$), and several sizes of disturbance—the set of disturbance sizes ($\sum p_{k(t)}$).

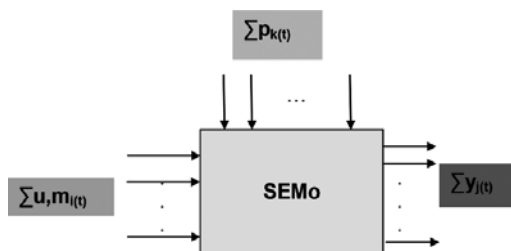**Figure 6** shows a schematic diagram of ecometallurgic multivariable system (SEMu).

Figure 6. The schematic diagram ecometallurgic multivariable system (SEMu). Source: [5]. $\sum u, m_{i(t)}$—the set of input quantities; $\sum y_{j(t)}$—the set of output quantities; and $\sum p_{k(t)}$—the set of disturbance sizes.

4. About the ecological balance

The concept of ecological balance was among the first to go beyond theoretical scientific studies, becoming an emblematic concept of harmony in the environment.
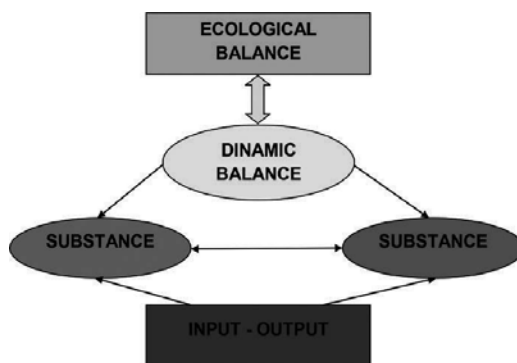
Figure 7. The scheme of the concept of ecological balance. Source: own research.

Ecological balance is a state (an ecosystem) maintained through complex interactions, which aroused particular interest deceleration in terms of theoretical debates and empirical observations.

The study of mechanisms that ensures this status allows the forecast *ecosystem* responses to disturbance anthropic. In terms of exchange of substance and energy, ecological balance expresses *the dynamic balance* ratio between input and output unit.

Figure 7 shows an illustration of the concept of ecological balance.

The maintaining of the ecological balance requires a self as finite nature of resources or space and a virtually unlimited potential of biological breeding populations.

The solutions for maintaining the ecological balance are the recycling and control of the growth which in the ecosystem leads to differentiation of functions for each population, followed by the creation of interdependence and organization of a self-regulating cybernetic system.

5. The principles for the environmental legislation applicable to ensure ecological balance

Among these principles, we consider useful to remember the following:

- The principles of the environmental legislation internally:

- The principle that environmental protection should be an essential element of economic and social policy of the state

- The principle of preventing environmental risks and damage occurrence—this principle has as its main goal to minimize environmental risks, including those from the effect of greenhouse gases.

- The principle of health priority compared with other purposes for use of natural resources—according to this principle greenhouse gases have a major harmful effect upon health.

- The precautionary principle in decision making—any decision, both in technology and in the environmental domain, should rely on this principle of precaution.

- The principle of prevention, reduction, and integrated pollution control—prevention must prevail in any ecological action; in the field of greenhouse gas many decisions of the European Union, which are binding for România as well, predict the slow and gradual decrease in quantity of the emissions and immissions of these gases available before 2030.

- The principle of retention of pollutants at source—the application of this principle is of particular importance to reduce the amount of greenhouse gas emissions.

- The principle of public participation in the environmental protection and improvement.

- The principle of conservation of biodiversity and of ecosystems specific to the natural biogeographical.

- The polluter pays principle—the principle of liability and polluter; this principle, by its punitive character has positive effects including a significant reduction in the quantity of greenhouse gases.

- The principle of state liability and accountability—this principle warns the authorities agaist possible penalties, including the noncompliance requirements on greenhouse gas emissions.

- The principle of sustainable use of the natural resources—the application of this principle implicitely leads to significant reductions in the quantity of greenhouse gases.

- The principle of cooperation in the context of relationship between state, society, and the environment user.

- The principle of the development of international cooperation for environmental protection —this principle takes into account the fact that greenhouse gases know no borders, so from this point of view, international cooperation in environmental protection becomes crucial.

- The principle of integrating environmental policy into other sectoral policies.

- The principles of external environmental legislation.

- The principles of "sic utere tuo".

- The principle of good neighborliness—the application of this principle has direct positive effects in default protection of neighboring countries, including in the area of greenhouse gas emissions.

- The principle of protecting the common heritage of mankind—significant reduction in the quantity of greenhouse gases provides the best conditions to accomplish this principle.

- The principle prohibiting pollution—this principle puts in the foreground the significant reduction of greenhouse emissions and imissions gas.

- The principle of protecting natural resources and common areas—greenhouse gases through their effect contradict this principle; consequently, the accomplishment of this principle implies a significant reduction on the amount of these gases.

These principles are particularly important for ensuring ecological balance. Unfortunately, we must recognize that their application is deficient and therefore their effectiveness remains largely theoretical.

6. Analysis of ecological electric arc furnace (EAF)

Electric arc furnaces are large generators of emissions, with a strong impact on the environment. The main emissions are as follows:

- Powders (powders) resulted during loading operations of raw materials, smelting, refining, alloying, evacuation steel containing heavy metals (Cr, Ni, Zn, Pb, etc.) that may reach values exceeding 15 kg/t steel.

- Process gases smelting and refining, containing mainly CO, CO_2, SO_x, and NO_x.

Of the total dust emissions, 90% are generated during smelting and refining operations. These powders are rich in oxides of iron, manganese, silicon, and aluminum and heavy metals such as nickel, chromium, cadmium, lead, and copper. But their chemical composition is highly variable, being directly influenced by

- composition of raw materials that make up the load EAF;

- melting driving mode;

- refining process used (oxygen gas or ore);

- during smelting and refining processes;

- steel grade that are elaborated.

Table 1 gives the range of variation of the chemical composition of the dust generated during the production of steel in electric arc furnaces in the United States and Germany, the load entirely made up of scrap.

No.	Component	Variation limits (%)		
		USA	Germany	
			Nonalloy steel	Alloy steel
1.	Fe$_{total}$	16.4–38.6	21.6–43.6	35.3
2.	Si	0.9–4.2	0.9–1.7	17.0
3.	Al	0.5–6.9	0.1–1.5	[a]
4.	Ca	2.6–15.7	6.6–14.5	0.4
5.	Mg	1.2–9.0	1.0–4.5	1.2
6.	Mn	2.3–9.3	0.9–4.8	2.0
7.	P	0.0–1.0	0.1–0.5	[a]
8.	S	0.0–1.0	0.3–1.1	0.1
9.	Zn	0.0–35.3	5.8–26.2	1.4
10.	Cr	0.0–8.2	0.0–0.1	13.4
11.	Ni	0.0–2.4	[a]	0.1
12.	Pb	0.0–3.7	1.3–5.0	0.4

[a]Lack of data. Source: [12]

Table 1. Chemical composition of EAF dust emissions.

In terms of the pollution decreasing, the crucial issue in the electric arc furnace is improving the collection of dust from the process gases both in the oven and work area for improved working conditions in those areas and to respect the limits imposed by legislation labor safety and environmental protection.

Determinants of the above requirements along with increased performance CAE, involves the following:

- expanding gas collection;

- increasing the separation or reduction of the dust content in the gas;

- reducing operation costs by reducing specific energy consumption;

- reducing maintenance costs and investment costs;

- protection against noise;

- improving working conditions.

To stop emissions from falling into the halls' working atmosphere and environment, electric arc furnaces had to be equipped with efficient capture and treatment.

This was also imposed by severe laws in many countries, on breakpoints dust, as shown in **Table 2**.

Country	France	Germany	Norway	Spain	Denmark
Allowable dust limit value (mg/m³$_N$)	10	20	25	50	2–5

Source: [12].

Table 2. Limit values for permissible concentrations of dust.

No.	Emission type	Technological phase of the processing	Emission percentage (%)
1.	Primary	Melting	93
2.	Secondary	Loading	2.75
		Evacuation	3.5
		By leaks (door, bowl—vaulted space around the electrodes)	0.75
	Total	Batch duration	100

Source: [12].

Table 3. Weight classification and dust emissions at CAE.

Emission of dust generated during the technological stages of a batch is divided into primary and secondary emissions in the order of their weight in the total amount of dust generated throughout the batch (see **Table 3**).

		Steel type			
No.	Heavy metals	Carbon steel		Inox steel	
		Offset variation (g/t)	Recommended value (g/t)	Offset variation (g/t)	Recommended value (g/t)
1.	As	0.06–0.14	0.1	0.01–0.02	0.015
2.	Cd	0.05–1.5	0.25	0.05–0.09	0.07
3.	Cr	0.3–2.0	1.0	12–18	15
4.	Cu	0.3–1.0	0.8	0.3–0.7	0.15
5.	Hg	—	0.15	—	0.15
6.	Ni	0.1–0.6	0.25	3–6	5
7.	Pb	5–20	14	1–3	2.5
8.	Be	—	0.05	—	0.05
9.	Zr	20–90	50	4–9	6

Source: [12].

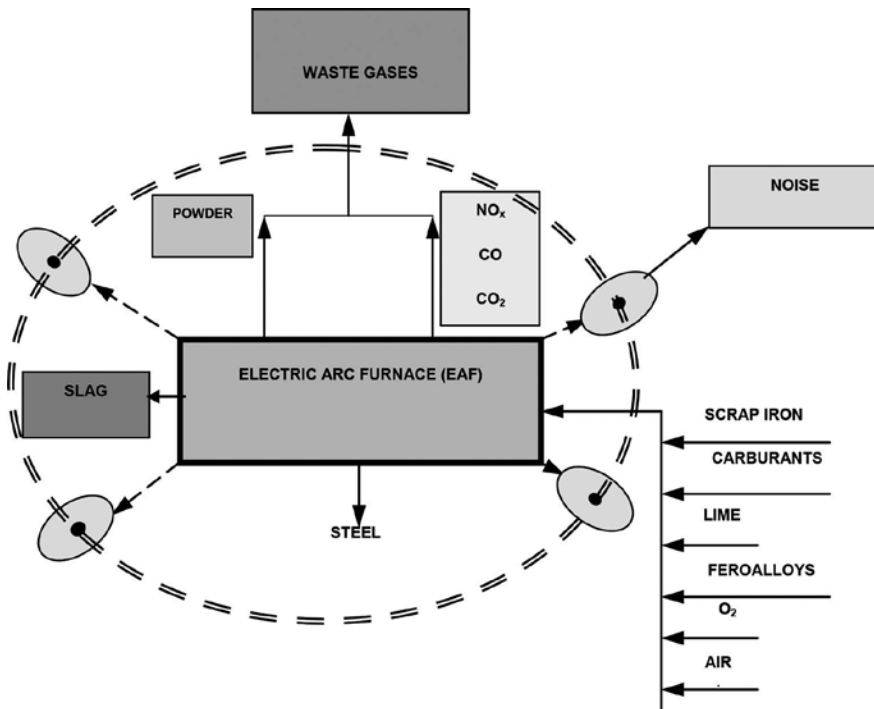**Table 4.** Emission factors for heavy metals in developing the CAE.

Figure 8. Scheme system of environmental pollution through EAF. Source: own research.

Gaseous phase of emissions that are emitted from the furnace is not only mainly composed of components: CO, CO_2, NO_x, and SO_x, but it also contains other very toxic ones, such as volatile organic compounds (dioxin and derivatives chlorinated benzene and phenol) resulting from burning organic oils that pollute the raw material.

Emission factors in the development of heavy metals in the arc furnace oscillate in a broad difference of values, recommending ATMOS PARCOM work for Europe values shown in **Table 4**.

In **Figure 8**, we present the main scheme of the environmental pollution system through CAE.

For dedusting flue gas discharged from the EAF, it is necessary to perform successively two categories of processes;

- capturing flue gas;

- dedusting flue gas itself.

Capturing the flue gas can be achieved mainly by

- Hoods;

- Suction canopy (the fourth hole in the roof of the furnace);

- Mixed (hood + the fourth hole in the ceiling).

Flue gas dust removal system can be:

- Moist by gas scrubbing;

- Centrifugal cyclone;

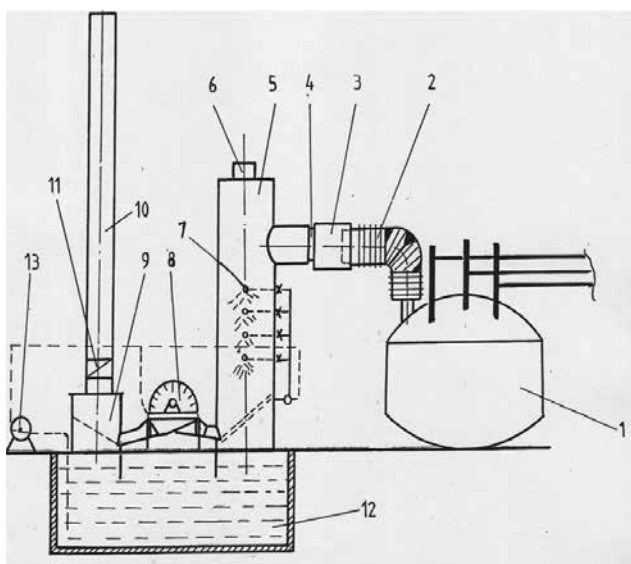- Type filters by using filter bags (textile) or electrostatic precipitators.

Figure 9. Cyclone wet (electric arc furnace 10 t). Source: [12]. 1—electric arc furnace; 2—suction; 3—mobile sleeve; 4—slot; 5—cooler; 6—tubing safety; 7—spray nozzles; 8—radial disintegrant; 9—separator; 10—cart; 11—throttle; 12—pool; and 13—pump.

The decision on the type of process and the type of facility used for dedusting flue gas discharged from the electric arc furnace is taken mainly based on the following criteria:

- to not adversely affect the process;

- the possibility of grouping the available space;

- keeping a smooth environment;

- operational safety;

- minimum investment volume;

- minimum operating cost;

- capitalization of substances treated.

An example of a wet cyclone used in an electric arc furnace of 10 t is shown in **Figure 9**.

The solution was gas suction through a fourth hole in the roof, proving to be the best way of capturing an electric arc furnace gas.

The suction pipe [2] provided with cooling fins was fixed by the metal construction of the vault of the oven so as to be able to follow all the movements of the tilting and swinging thereof.

Between suction and fixed air purifying, there is a mobile sleeve [3] and a space (gap) [4] necessary both for taking thermal expansion and for regulating the flow of cold air sucked.
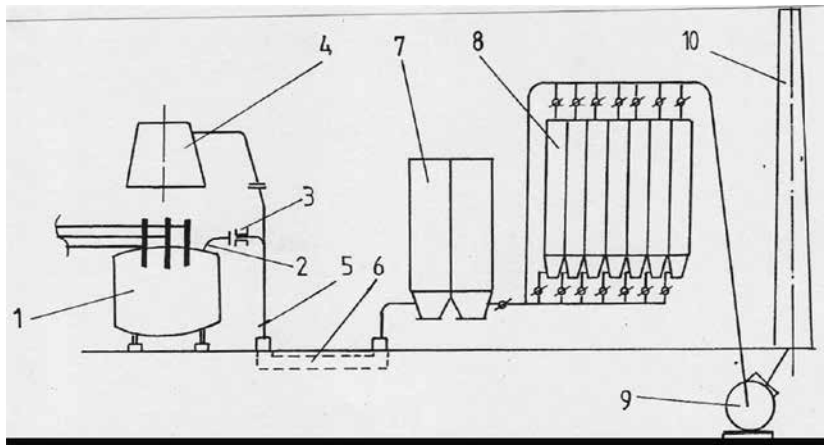

Figure 10. Scheme cyclones exhaust gases from the electric arc furnace (EAF). Source: [12]. 1—electric arc furnace; 2—suction; 3—chamber; 4—mobile hood; 5—keyboards; 6—underground channel; 7—cooler; 8—battery filters; 9—turbo-fan (common); and 10—cart.

The burned gases are cooled entirely up to their dew point in the cooler [5] by spraying water through four nozzles [7]. The cover of the cooler is equipped with a safety pipe [6] for additional entry of air.

The Radial disintegrator [8] is arranged downstream of the gas cooler and extracts therefrom, acting as a suction fan, where a fine treatment takes place at the same time. The gases then enter tangentially into a water separator [9] and are discharged into the atmosphere through a stack [10].

The wash water is recycled to the cyclone reactor. From a pool of water [12] 18 m^3, various points of use are fed by a pump.

The dedusting process of exhaust gases from electric arc furnaces (IPROMET solution) envisages:

• mixed solution for collecting the gaseous phase, both by the fourth hole in Olt (provided with a fitting cooled) and through a mobile hood over the furnace and electric drive (for secondary emissions capture);

• an air cooling gas at ambient temperature;

- filter element—bag filter;

- depression necessary to ensure—through an exhaust chamber (both for the fourth hole in the vault and the vault).

Figure 10 presents the scheme of dedusting plant exhaust gases from the electric arc furnace, used in Romanian steelworks.
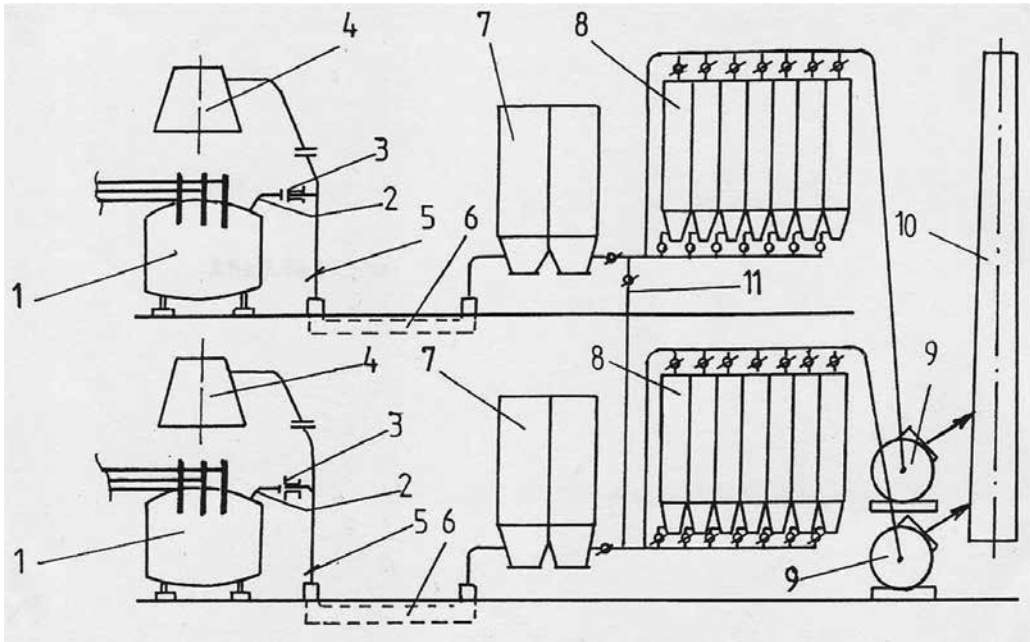

Figure 11. The system of scrubbers in parallel. Source: [12]. 1—electric arc furnace; 2—suction; 3—chamber; 4—mobile hood; 5—flap; 6—underground channel; 7—cooler; 8—battery filters; 9—exhaust; 10—cart; and 11—valve switching.

The flue gases collected through both of the fourth hole in the roof of the oven and the suction pipe (2), gas ceding their heat of reaction in the combustion chamber (3) and through the hood furniture (4). They are directed to an adjustable flap pressure (5) underground channel (6). From this channel, the gases are cooled in cooler (7) and then filtered through the filters battery (8) with bag filters (fabric).

The depression necessary to collect and circulate the gas is ensured by the suction blower (9) and the output bin (10), and the gases are directed after being dedusted.

Aspirations of false air (both by adjustable gap upstream of the combustion chamber and the other leg) directly influence the efficiency of the furnace exhaust gas capture (increased false airflow aspirated gas flow mitigates captured).

Treatment plant may be individual (for each furnace) or in parallel (coupled two by two), each serving one furnace, as shown in **Figure 11**.

Through the throttle switch (11), one can reverse the serviced furnace or that cyclone operation. The coupling system of the plants has the advantage of using a single cyclones for the two furnaces (not simultaneously) so that during repair (revision) of the installation, one of the two furnaces can be operated by the cyclone operation.

Using cyclone influences the regime of the pressure in the oven. Correlated to the increase in false sucked airflow (and implicitely exhaust gas discharged from the oven) caused by the wear dome oven, this requires the use of vaults and cooled walls.

Intensifying the thermal oven and its best possible sealing are goals that lead both to the increase of productivity oven and to reducing specific energy consumption, and they should be made to avoid the risk of uncontrolled ignition of the gas phase route cyclones. To this end, the introduction of the combustion chamber has a decisive role.

In the case of dusting with electrical filters, the gas passes through the electrofilter chamber where deposition electrodes, linked to the ground, and emission electrodes are placed. Due to the difference of voltage of about 75–100 kV between emission electrodes of negative polarity and deposition electrodes, of positive polarity, an electrostatic field is formed.

In the vicinity of the emission electrode, a strong failure of potential is established, which produces the ionization of the gas in this area. Positive ions remain on the emission electrode and the electrons move to the deposition electrodes. on their way The electrons meet gas molecules and dust particles which they ionize negatively. These ionized particles adhere to the deposition electrodes they meet.

The layer of powder deposited can reach a thickness up to 10 mm. It is removed by shaking the deposition electrodeswith the aid of a striking hammer device. Dust collection is achieved in a specially arranged bunker at the bottom of the electrostatic precipitator.

In electric filters, continuous current is used so that the ionized particles travel only in one direction (toward the deposition electrodes).

7. Pollution prevention through afterburner

As shown, after thermal metallurgical processes gaseous combustible substances such as CO, H_2, and CH_4 result. It is proposed that these gases be used, after leaving the contour energy as substitutes for other aggregates of expensive or deficient fuels.

Lately, to increase the efficiency of enthalpy and chemical potential (thermal effect of oxidation reactions—burning) of burnt gas, one need to burn combustible components in the working unit of the aggregate.

This process of modernization, applied, for example, to oxygen converters and electric arc furnace (EAF) is called postcombustion. Since the consumption of CO takes place inside, the method is also considered a way of reducing pollution.

Essentially, the method involves the recovery, even in the technological outline, of the heat of exothermic combustion reaction of CO with oxygen, blown into the workspace via a lance especially designed for this purpose:

$$(CO)_{g.a} + O_2 \rightarrow (CO_2)_{g.a} + Q \tag{1}$$

The process efficiency is assessed by postcombustion indication rate, defined as the ratio indicator:

$$\eta_{p.c} = \frac{(\%CO_2)}{(\%CO + \%CO_2)} \tag{2}$$

Detailed analysis of postcombustion process shows that there are still reservations regarding the technical possibilities for improvement and contributions to the development of theoretical knowledge underpinning the process.

Thus, the materials published so far have failed a systematized existing information. For this reason, the authors of this paper, proposes the following classification of postcombustion processes.

a) Natural postcombustion, in which extra energy is built on the combustion components (CO and H_2), naturally eliminated from the process; combustion occurs upon contact with the jet of oxygen blown into the furnace. This process has two options:

(a.1) Natural free postcombustion based on the furnace burning combustible gases from process gases in the presence of oxygen jet blew right through the walls of the unit, and depending on the placing of the jet, we identify two technologies:

• Natural free postcombustion with nonimmersed jet or, in short, postcombustion nonimmersed jet where the postcombustion is produced in the white space of the melt-existing fireplace.

• Natural free postcombustion with immerged jet or, in short, postcombustion immersed jet, in which case the oxygen jet pierces the layer of slag, producing foaming slag, which is why the process is also found under the postcombustion foamed slag.

(a.2) Forced natural postcombustion performed when the fireplace blows a jet of supplemental oxygen crossing metal melt and slag;

b) Artificial postcombustion that involves blowing of a coal jet and a jet of oxygen at the same time. In this case, postcombustion also involves burning coal and related processes.

c) Combined postcombustion, which involves a combination of the above.

In specific literature, postcombustion is analyzed as the process that occurs in conjunction with other measures (oxy-combustion, foamed slag, etc.). Therefore the authors consider it necessary to distinguish between:

- pure postcombustion, which means postcombustion in a classic oven without other measures;

- pseudo-postcombustion, where postcombustion relates to other modernizing processes.

Since in the case of CAE, there may be hydrogen gas, H_2 coming from the combustion of hydrocarbons added in the combustion process or waste scrap, and it is possible to have a postcombustion reaction:

$$H_2 + \frac{1}{2} \cdot O_2 \rightarrow H_2O \tag{3}$$

In these circumstances, we propose that for the calculation of efficiency of postcombustion to use a new relationship that will characterize the complete process:

$$\eta_{p.c.c} = \frac{(\%CO_2 + H_2O)}{(\%CO_2 + \%H_2O + \%H_2 + \%CO)} \tag{4}$$

Based on the general theory of thermo metallurgical installations, CAE part of, we know that when combustible substances (such as CO, H_2, and CH_4) are burnt with flame, a process of dissociation of products of combustion simultaneously occurs, according to the reactions :

$$CO_2 \rightarrow CO + \frac{1}{2} \cdot O_2 - Q_1$$
$$H_2O \rightarrow H_2 + \frac{1}{2} \cdot O_2 - Q_2 \tag{5}$$

This phenomenon makes a distinction between combustion calorimetry temperature given by the equation:
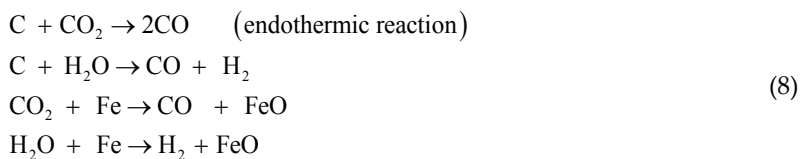
$$t_k = \frac{H_i}{v_{g.a}c_{p_{g.a}}} \tag{6}$$

where H_i is the calorific value of the fuel [J/kg; J/m^3_N]; vg.a—the amount of gas flared [m^3_N g.a/ m^3_N; kg] and—specific heat of flue gas [J/m^3_N] and theoretical combustion temperature:

$$t_t = \frac{H_i - Q_{dis}}{v_{g.a}c_{p_{g.a}}} \tag{7}$$

where Q_{dis} is the amount of heat consumed for the dissociation of CO_2 and H_2O [J/kg; J/m^3_N]. Theoretical calculations, confirmed by the experiment, show that this lost heat can have values $Q_{dis} = (2...4 \%)H_i$.

At the same time, postcombustion products CO_2 and H_2O can react with carbon and iron in molten metal or through oxidation with the iron in the charge:

$$
\begin{aligned}
&C \ + CO_2 \rightarrow 2CO \quad \left(endothermic\ reaction \right) \\
&C \ + \ H_2O \rightarrow CO \ + \ H_2 \\
&CO_2 \ + \ Fe \rightarrow CO \ \ + \ FeO \\
&H_2O \ + \ Fe \rightarrow H_2 \ + FeO
\end{aligned}
\tag{8}
$$

The last two observations lead to the conclusion that at the same time with the postcombustion processes there occur processes of endothermic consumption of the products CO_2 and H_2O. Based on this affirmation, in this paper, we propose that we generally call such a phenomena anticombustion.

Theoretical and experimental study in postcombustion shows that so far not enough consideration has been given to intensify postcombustion processes. One of the theoretical and practical possibilities of intensifying launched by the authors in the research is the postcombustion in ultrasonic field called postcombustion ultrasonic (PCU). This new method assumes that the jets of fluids (e.g., oxygen) blown into postcombustion zones be ultrasonic energy carriers, based on which the processes of mass and heat transfer in the mentioned area to be enhanced.

8. Conclusion

The metallurgical environmental complexity and therefore the Metallurgical Process Technology (MPT) is grounded and by which it interacts systems: The system-Energy-Recycling The Environment (ERE), Ecological system (ECO), Recycling, Reclamation the system (REC-REV).

The concepts of sustainable development (SD) and the total quality (TC) are of particular importance in analyzing correlations between the System Technology Process Metallurgy (MTP) and the other systems.

The Metallurgical Ecosystem analysis has as a starting point ecometallurgic monovariable system (SEMo). This system applies only theoretically, and it is very important for modeling and simulation environment related to metallurgical processes.

The ecological balance is a concept very complex and very difficult.

The especially self-regulating mechanisms and applying to the concept of sustainable development is very important for ensuring ecological balance.

The principles of environmental legislation were also of particular importance for achieving ecological balance. Among these principles we mention: the principle of preventing environmental risk and damage, the principle of priority health compared with other purposes for use of natural resources, the principle of prevention, reduction, and integrated pollution control, the principle of retention of pollutants at source, the principle of public participation in the protection and improving the environment.

Dedusting the flue gas discharged from the electric arc furnace (EAF) has a special significance for its hipopolluting functioning. The main categories of processes to achieve this are flue gas capture and dedusting actual flue gas.

From a wide range of machinery and equipment specific to this field, having as starting point the scheme of system environmental pollution through EAF, in this first part of our article, we presented the cyclone of wet and dry dedusting plant.

The technological development of steel in electric arc furnaces (EAF) is one that is ecologically impaired. The emissions and immissions resulting from this technological process are many and in significant amounts. In conclusion, special care is required from production managers (and not only) to ensure hipopolluting operation conditions of EAF. This concern should begin in the early stages of research both in technology development and designing this complex aggregate.

Achievements in greening the operation of the electric arc furnace (EAF) to develop steels, are relatively modest on a national level.

The costs for installation and commissioning of the capture and treatment of this complex aggregate emissions are significant. Even so, the restrictive environmental regulations in the field constantly force the user to take technological measures to ensure the functioning of hipopolluting EAF.

From this point of view, the specialists in the field should pay far greater attention and importance of scientific research and design.

Author details

Adrian Ioana[*] and Augustin Semenescu

*Address all correspondence to: adyioana@gmail.com

University Politehnica of Bucharest, Bucharest, Romania

References

[1] Brimacombe, L., Jackson, C., Schofield, N., Artificial intelligence expert systems for steelworks pollution control, La Revue de Métallurgie-CIT Janvier 2001, pp. 111–116, 2001.

[2] Bardet, I., Desmonts, T., Ryckelynck, F., Bourrier, Ph., Video monitoring of visible atmospheric emissions: from a manual device to a new fully automatic detection and classification device, La Revue de Métallurgie-CIT 2000, pp. 1223–1234, 2001.

[3] Ioana, A., Metallurgy's Impact on Public Health, Review of Research and Social Intervention, 43/2013, ISSN: 1583-3410, eISSN: 1584-5397, (ISI-Web of Social Science/ Social Science Citation Index Expanded), Accession Number: WOS: 000328004800011, IDS Number: 266DY, pp. 169–179.

[4] Ioana, A., Semenescu, A., Technological, economic, and environmental optimization of aluminum recycling, Journal of the Minerals, Metals & Materials Society, JOM, 65, 8 (2013), ISSN: 1047-4838 (ISI-Web of Science/Science Citation Index Expanded), Accession Number: WOS: 000322136400007, DOI: 10.1007/s11837-013-0664-6, IDS Number: 187RN, pp. 951–957.

[5] Ioana, A., Elemente de Automatizare Complexă a Sistemelor Ecometalurgice (ACSE) şi de Robotizare, Editura Printech, ISBN: 978-606-23-0246-7, Bucureşti, 2014.

[6] Nicolae, A., Scorţea, C., Lepădatu, Gh., Sisteme ERE (environment-recycling-energy) în industria siderurgică, Editura Fundaţia Metalurgia Română, Bucureşti, 1997.

[7] Ioana, A., Semenescu, A., Preda, C.F., Knowledge management innovation for sustainable development in the context of the economic crisis, WSEAS ISI Proceedings of the 2013 International Conference on Environment, Energy, Ecosystems and Development (EEEAD 2013), Venice, Italy, September 28–30, 2013, pp. 21–26, ISBN: 978-1-61804-211-8.

[8] Ioana, A., Mirea, V., Bălescu, C., Analysis of service quality management in the materials industry using the BCG matrix method, Amfiteatru Economic Review, XI, 26, 2009, pp. 270–276, [ISSN: 1582-9146, ISI-Web of Science/Science Citation Index Expanded], Bucureşti, 2009. Accession Number: WOS: 000267351800004, IDS Number: 462KQ, Research Areas: Business & Economics Web of Science Categories: Economics, Publisher Editura ASE, Piata Romana, Cited References in Web of Science Core Collection: 8,Times Cited in Web of Science Core Collection: 2.

[9] Ioana, A., Bălescu, C., Environmental study of the formation of evacuated burnt gases from a steels making plant, Revista De Chimie 5/2009, pp. 468–471, [ISSN 0034-7752, ISI-Web of Science/Science Citation Index Expanded], Bucureşti, 2009. Accession Number: WOS: 000267459400008, IDS Number: 463VB, Research Areas: Chemistry; Engineering Web of Science Categories: Chemistry, Multidisciplinary Engineering, Chemical, Publisher Chiminform Data SA, Bucureşti, Cited References in Web of Science Core Collection: 10.

[10] Ioana, A., Semenescu, A., Preda, C.F., Elements of best management for metallurgical technological plants, Metalurgia International 18(1/2013), ISSN 1582-2214, (ISI-Web of Science/Science Citation Index Expanded), Bucureşti, 2013, pp. 165–167. Accession Number: WOS: 000315368200037, IDS Number: 095XL, Research Areas: Metallurgy & Metallurgical Engineering, Web of Science Categories:Metallurgy & Metallurgical Engineering, Publisher EDITURA ŞTIINŢIFICĂ FMR, Bucureşti, Cited References in Web of Science Core Collection: 9.

[11] Ioana, A., Semenescu, A., Preda, C.F., Metallurgical marketing mix (MMM) elements, Metalurgia International, 18(1/2013), ISSN 1582-2214, (ISI-Web of Science/Science

Citation Index Expanded), Bucureşti, 2013, pp. 156–159. Accession Number: WOS: 000315368200035, IDS Number: 095XL, Research Areas: Metallurgy & Metallurgical Engineering, Web of Science Categories: Metallurgy & Metallurgical Engineering, Publisher EDITURA ŞTIINŢIFICĂ FMR, Bucureşti, Cited References in Web of Science Core Collection: 10.

[12] Ioana, A., Nicolae, A., Predescu, Cr., Sandu, I.F., Sohaciu, M., Calea, G.G., Conducerea Optimală a Cuptoarelor cu Arc Electric, Editura Fair Partners, Bucureşti, ISBN 973-8470-04-8, 2002.

Edited by Andrew J. Manning

Greenhouse Gases - Selected Case Studies, is a book which covers a range of topics. The long term effective management of the natural environment, requires a detailed understanding of greenhouse gases. This has both environmental and economic implications, especially where there is any anthropogenic involvement. Numerical models are often the tool and framework used for predicting the effects, both in the long-term and short-term, of greenhouse gases. However, the relevant atmospheric processes can vary quite considerably depending upon the spatial and temporal scales under consideration. For this reason for the past few decades, scientists, engineers, meteorologists and mathematicians have all been continuing to conduct research into the many aspects which influence greenhouse gases. These issues range from: industrial science, agricultural research, carbon dioxide and other emissions. This book reports the findings from recent research in greenhouse gases, primarily in the the form of case studies, particularly from an interdisciplinary perspective. The research was carried out by researchers who specialise in areas such as: energy production, emissions from livestock, chemical industry, and metallurgical process technology.

IntechOpen